

Studying the interplay between plasmas and magnetic fields in the laboratory

P. Mabey^{1*}, B. Albertazzi¹, Th. Michel¹, G. Rigon¹, E. Filippov², E. Falize³, L. Van Box Som³, A. Ya. Faenov⁴, Y. Kuramitsu⁴, T. Matsuoka⁴, S. Makarov², N. Ozaki⁴, S. Pikuz², T. Pikuz⁴, Y. Sakawa⁴, F. Kroll⁵, F. Brack⁵, P. Perez-Martin⁵, A. Pelka⁵, K. Falk⁵, C. A. J. Palmer⁶, G. Gregori⁶, P. Tzeferacos⁷, D. Lamb⁷ and M. Koenig¹

¹LULI, France, ²JIHT-RAS, Russia, ³CEA-DAM-DIF, France, ⁴Osaka University, Japan, ⁵HZDR, Germany, ⁶University of Oxford, UK, ⁷University of Chicago, USA

paul.mabey@polytechnique.edu



Talk outline



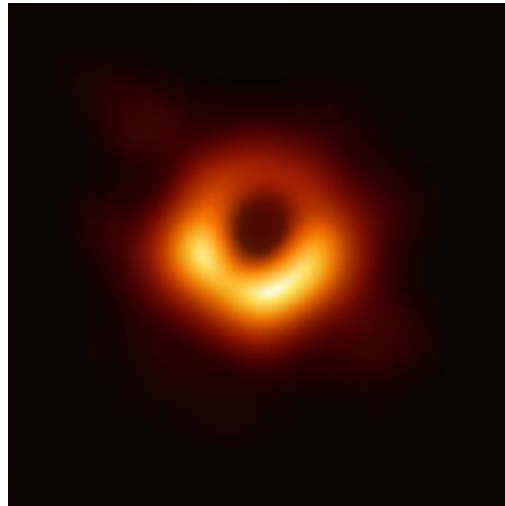
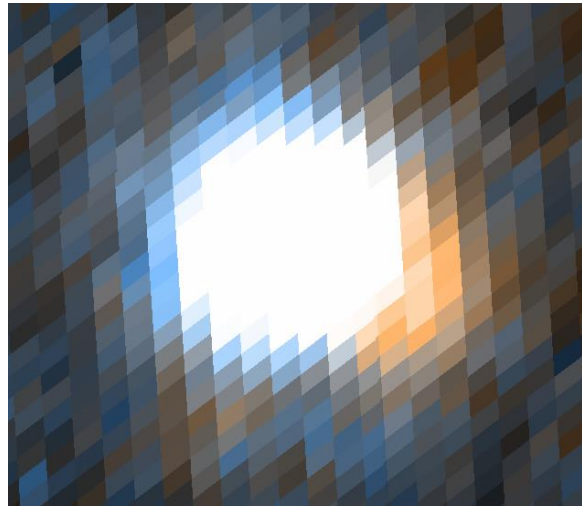
- What is laboratory astrophysics?
 - Magnetized accretion columns – POLAR project
 - Hydromagnetic shocks and supernova remnants
-

Talk outline



- What is laboratory astrophysics?
 - Magnetized accretion columns – POLAR project
 - Hydromagnetic shocks and supernova remnants
-

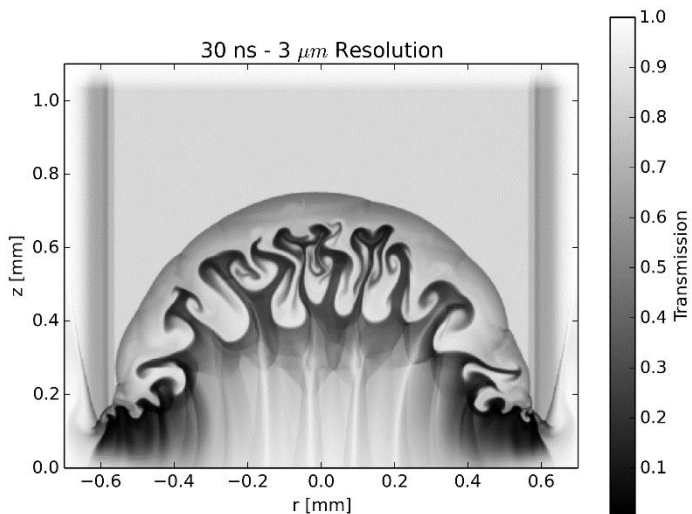
Observations and simulations are limited



Astrophysical observations are limited by the spatial resolution of our detectors and also the frequency or speed with which some phenomena occur.

(left) AM Herculis polar star, photographed in the UV range, by GALEX, CIT

(right) Black hole at the centre of Messier 87, by the Event Horizon Telescope



Numerical simulations contain approximations and can take impractically long to run

G. Rigon et al, PRE, E 100 (2), 021201, (2019).

High energy density science



Energy densities created by the interaction of a high-power laser with matter are roughly equivalent to those in many astrophysical systems ($> 10^{11}$ J/m³)

Three different regimes:

Identical (1:1 scale)

Gives physical information directly e.g. opacity, equation of state

Similar (1:10¹⁷ scale)

Gives physical information providing certain scaling criteria are met

Analogous

Scaling criteria not met but certain phenomena reproduced. Can be used to validate codes

Scaling laws



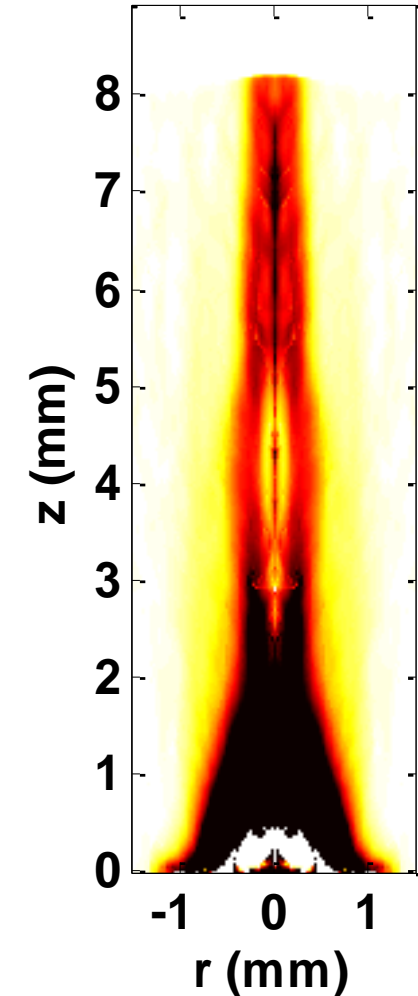
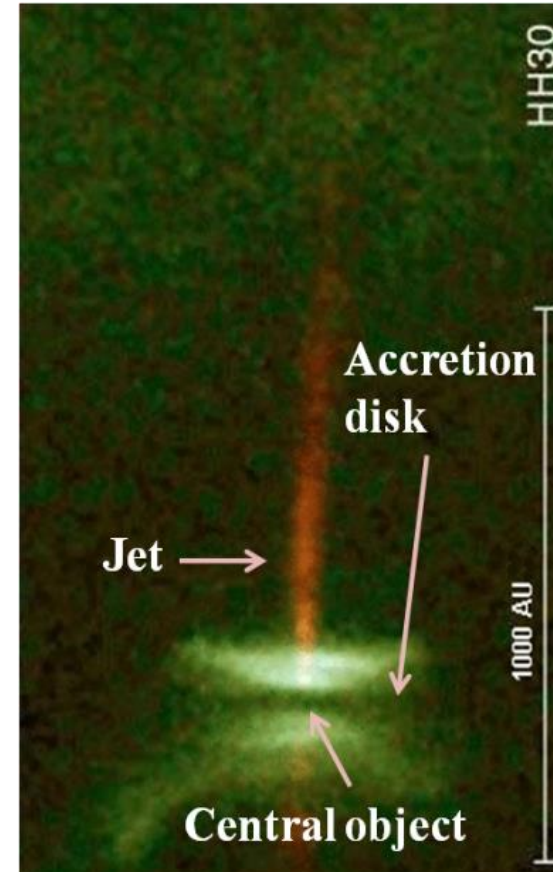
Hydrodynamic and MHD fluid equations can be recast as scale independent with the use of certain dimensionless numbers

(e.g. Mach number, Reynolds number, Boltzmann number, plasma beta etc...)

$$\mathbf{v} \rightarrow v_0 \mathbf{v}^*, \quad \mathbf{r} \rightarrow L_0 \mathbf{r}^*, \quad t \rightarrow \frac{L_0}{v_0} t^*, \quad \rho \rightarrow \rho_0 \rho^*, \quad P \rightarrow \rho_0 v_0^2 P^*$$

$$\rho^* \left(\frac{\partial \mathbf{v}^*}{\partial t^*} + \mathbf{v}^* \cdot \nabla^* \mathbf{v}^* \right) = -\nabla^* P^* + \frac{1}{\text{Re}} \nabla^{*2} \mathbf{v}^*,$$

Ryutov, *Astrophys. J.* 127, 465 (2000)



Astrophysical jet in the laboratory (B. Albertazzi et al. *Sci* (2014))

LULI2000



Situated on the Saclay plateau outside of Paris in Ile-de-France

Part of L'école Polytechnique (Institut Polytechnique de Paris)

Funded in parts by CNRS and CEA



LULI laser facility



MILKA target chamber

1 x 500 J, 1.5 ns, 2ω beam

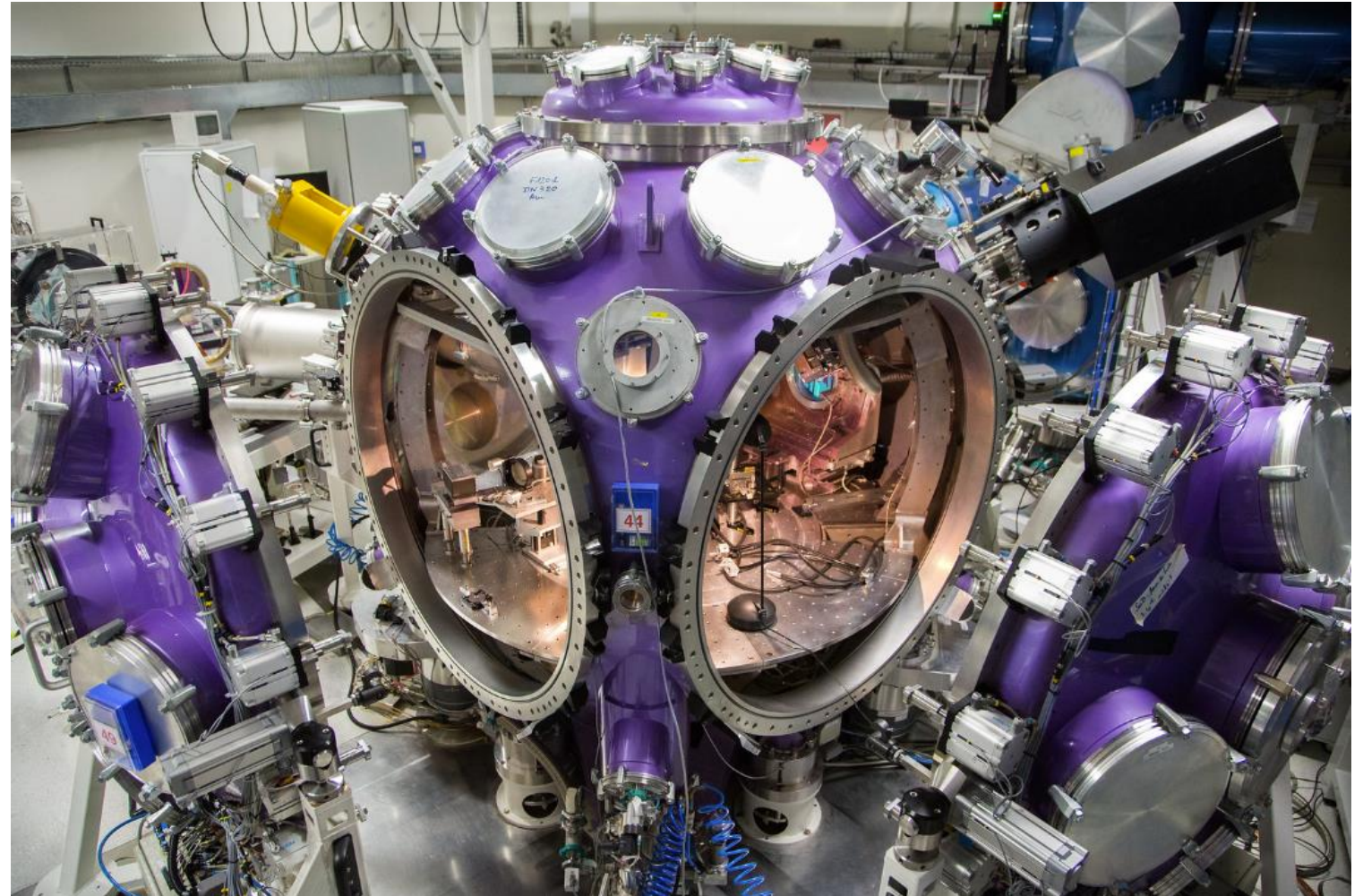
1 x 80 J, 10 ps, 1ω beam

1 x 1 mJ, 7 ns, 2ω optical probe beam

Pulsed power system

Capacitor-based pulse generator
charged to 9.6 kV, providing 23.6 kA to
a Helmholtz coil

Magnetic field reaches peak value after
183 μ s and stays constant for a period
of several μ s



Diagnostics



Emission

Streaked in time, 2-D, energy resolved, temperature calibrated, Zeeman splitting

Optical probe

Interferometry, schlieren, shadowgraphy, Faraday rotation

X-ray

Absorption spectroscopy, diffraction, radiography

Particle beam

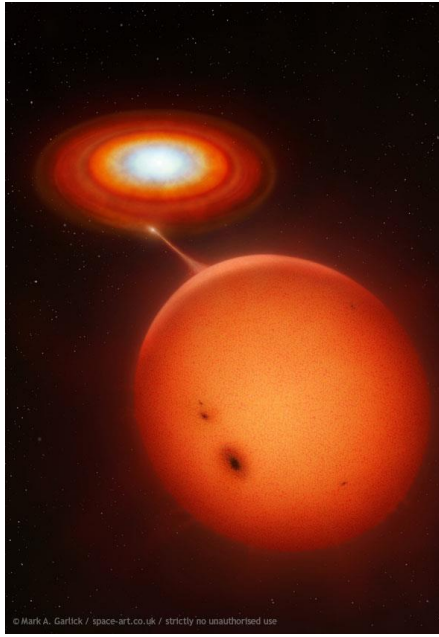
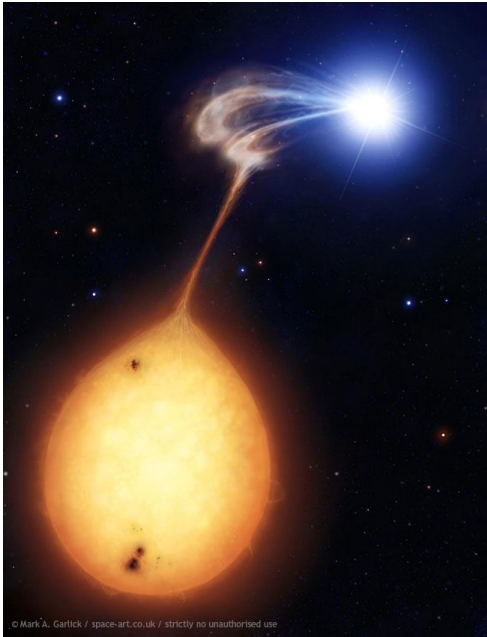
Deflectometry, stopping power, scattering

Talk outline



- What is laboratory astrophysics?
 - **Magnetized accretion columns – POLAR project**
 - Hydro-magnetic shocks and supernova remnants
-

What are Cataclysmic variables?



(left) Mark A. Garlick, Magnetic Accretion (1998)

(right) Mark A. Garlick, Cataclysm VI (2008)

Cataclysmic variables are semi-detached binary systems, containing a white dwarf and a companion star.

Non-magnetic (< 100 T)

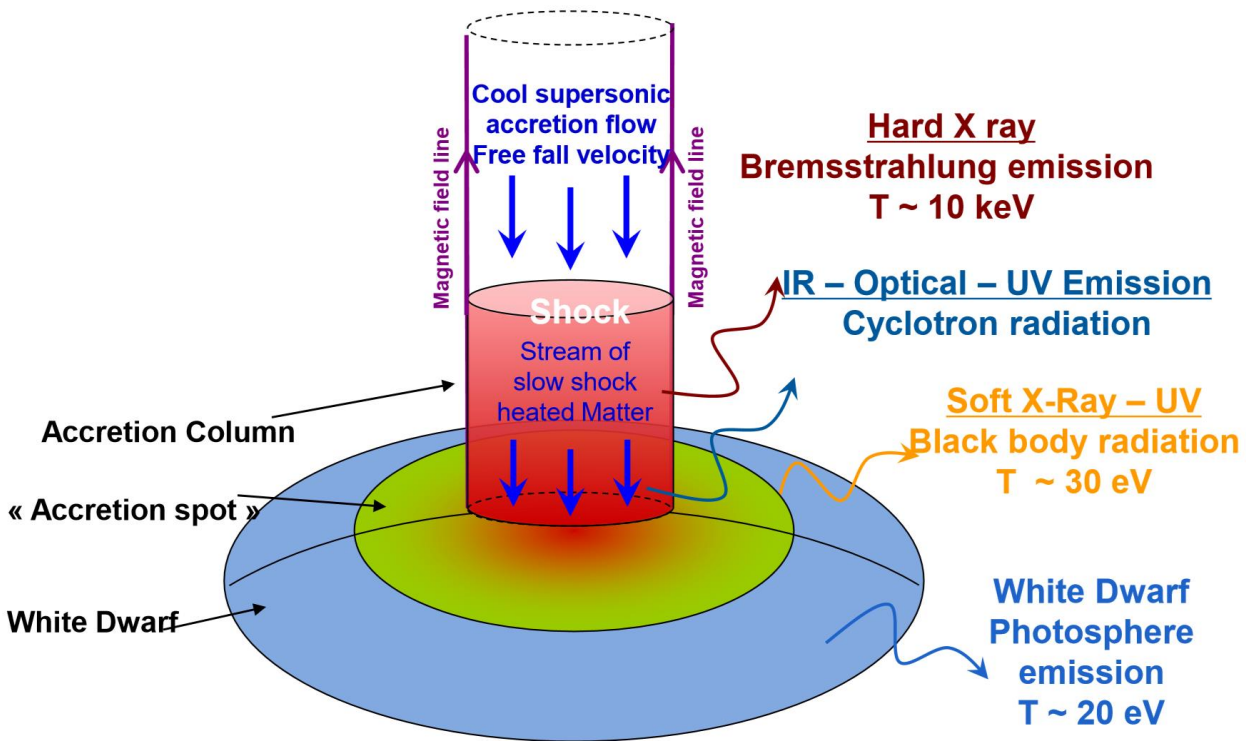
The white dwarf continuously draws matter from the companion star forming an accretion disk.

Magnetic (> 100 T)

The plasma flow is channeled by the magnetic field lines and accretes directly onto the white dwarf poles, leading to the formation of an accretion column.

Such systems are strong hard X-ray sources due to the formation of a stationary shock at the interaction point between the column and the white dwarf surface.

Outstanding questions surrounding MCVs



Adapted from Wu 2000, Spac. Sci. Rev. 93, 611

The only way to determine these objects' properties is based on fitting the observed X-ray flux and comparing to models or simulations.

Different approximations to treat radiation give different spectra.

They also disagree in the expected shock height.

Measuring the shock height is one possible way to constrain models.

Observed quasi-periodic oscillations in the luminosity of these systems are currently poorly understood.

Experimental setup



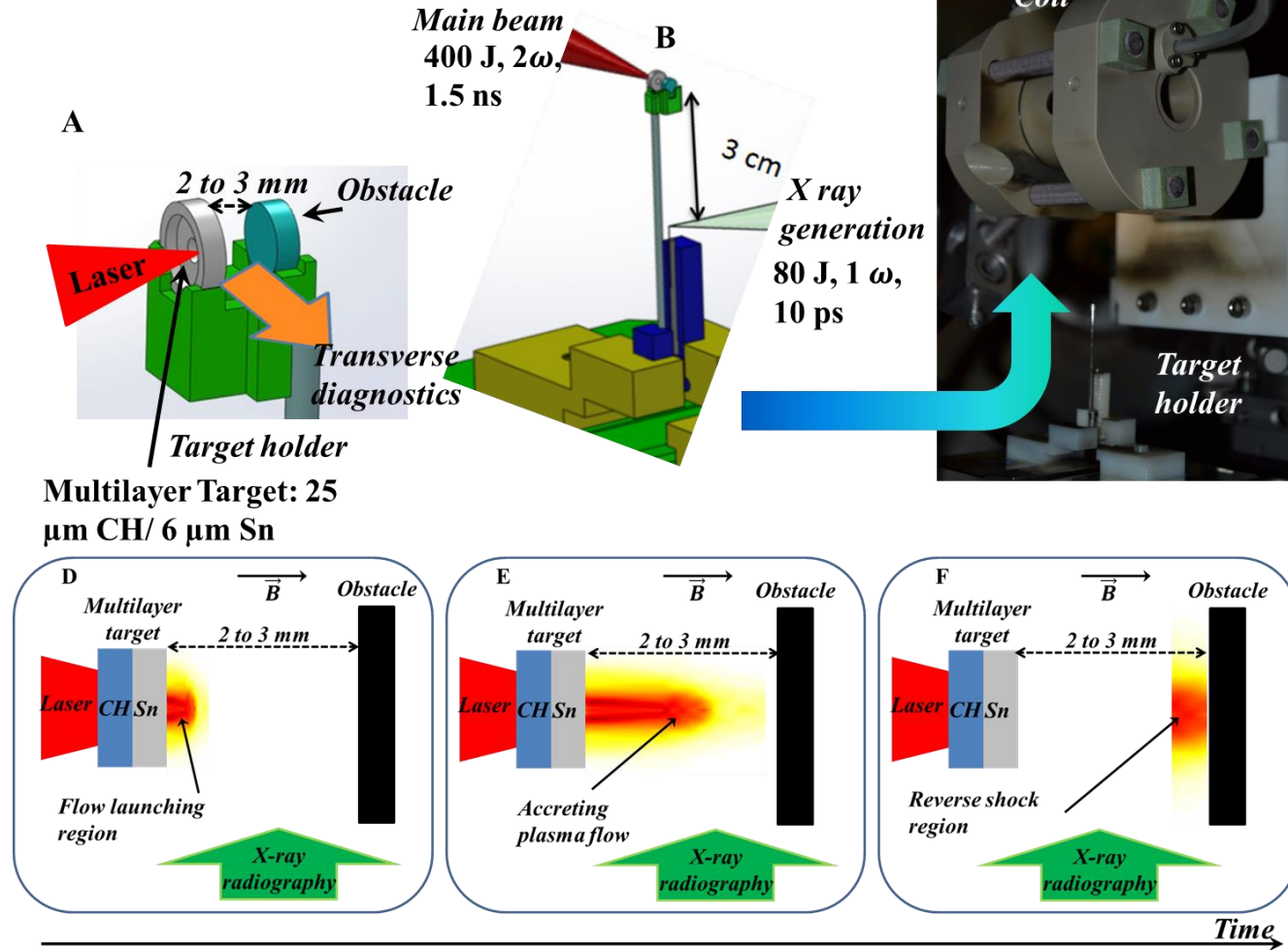
Nanosecond laser used to drive plasma flow onto obstacle.

Optical diagnostics employed to observe propagation of plasma flow.

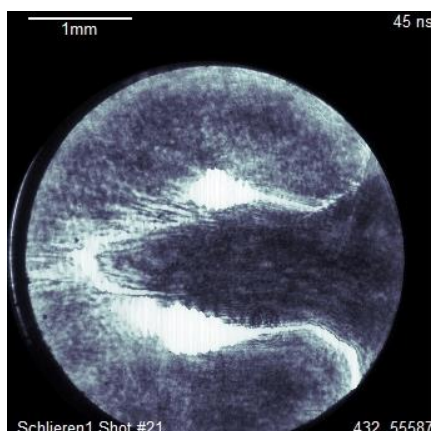
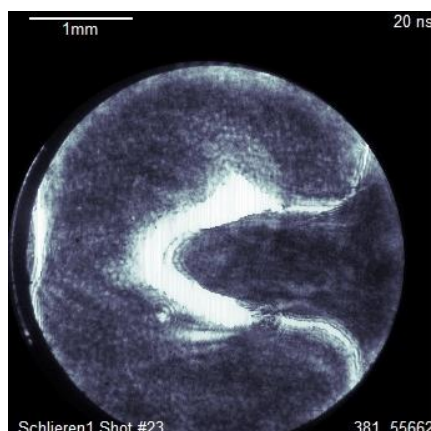
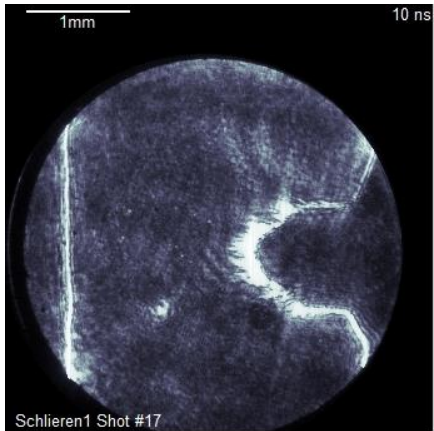
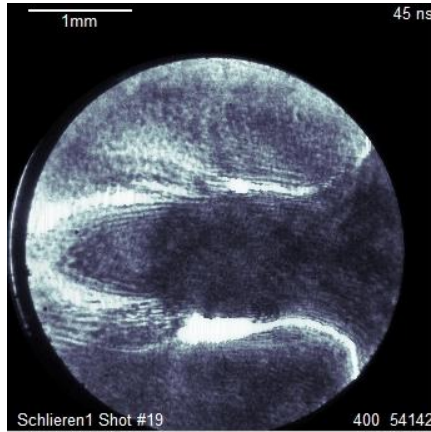
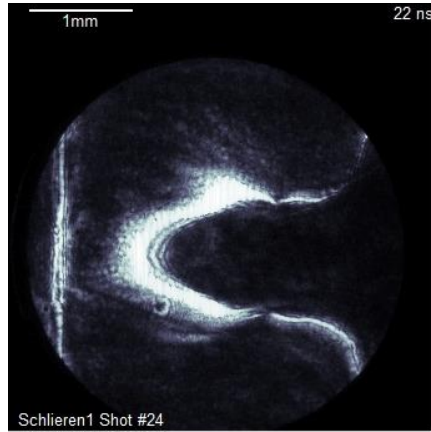
Picosecond laser used to generate X-ray source for radiography.

Whole setup placed in Helmholtz coil capable of producing 15 T magnetic field.

B. Albertazzi et al., HPLSE 6 e43 (2018)



Schlieren imaging results



0 T

Laser incident from the right hand side of the image. Plasma flow is driven from rear surface towards the obstacle on the left hand side.

15 T

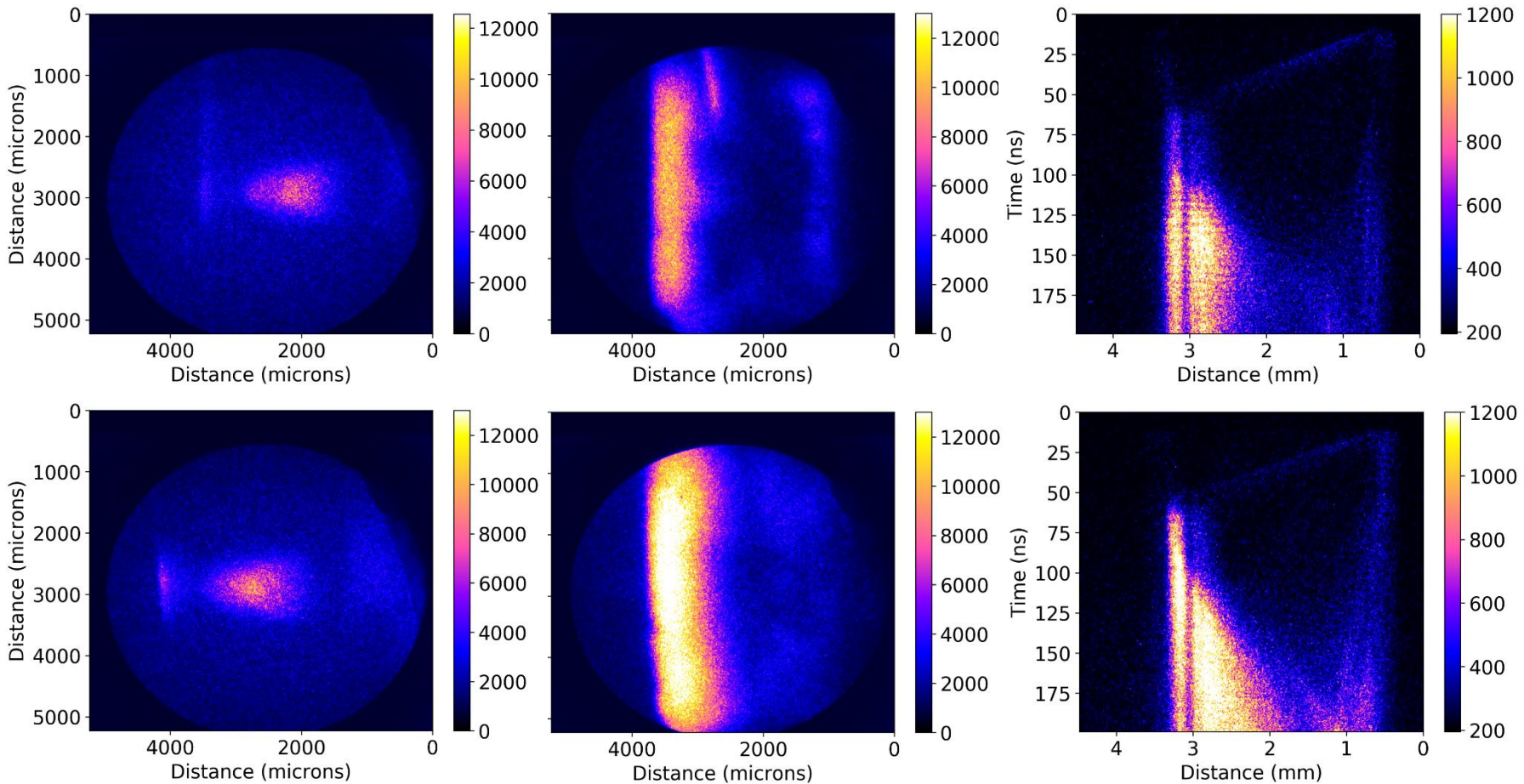
The density of the reverse shock region is higher than the critical value. No late times are recorded.

10 ns

20 ns

45 ns

Optical emission results



0 T

Laser incident from the right hand side of the image. Plasma flow is driven from rear surface towards the obstacle on the left hand side.

15 T

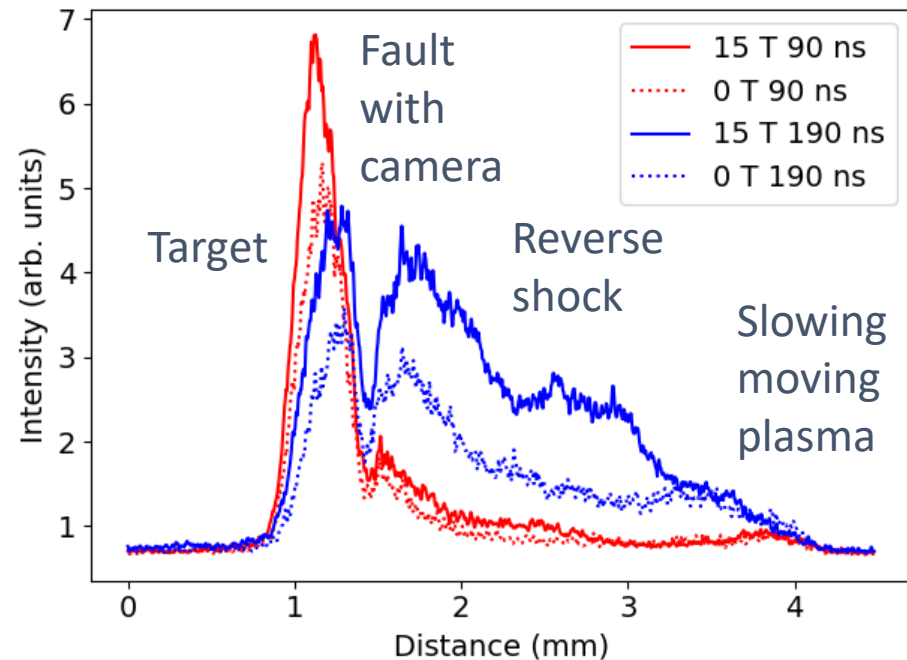
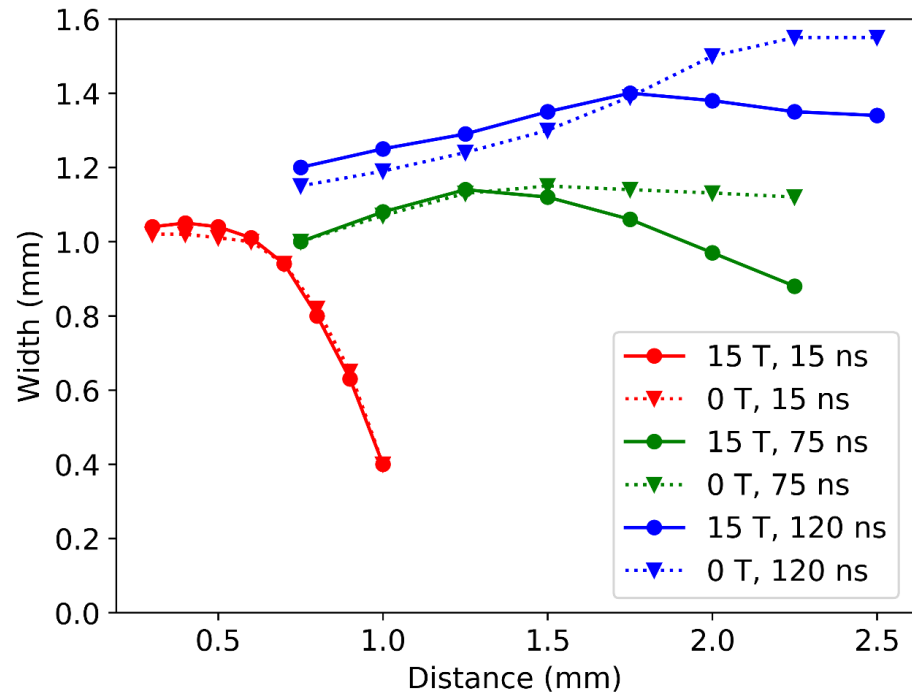
The emission profiles with and without the magnetic field vary greatly.

Pre-collision

Post-collision

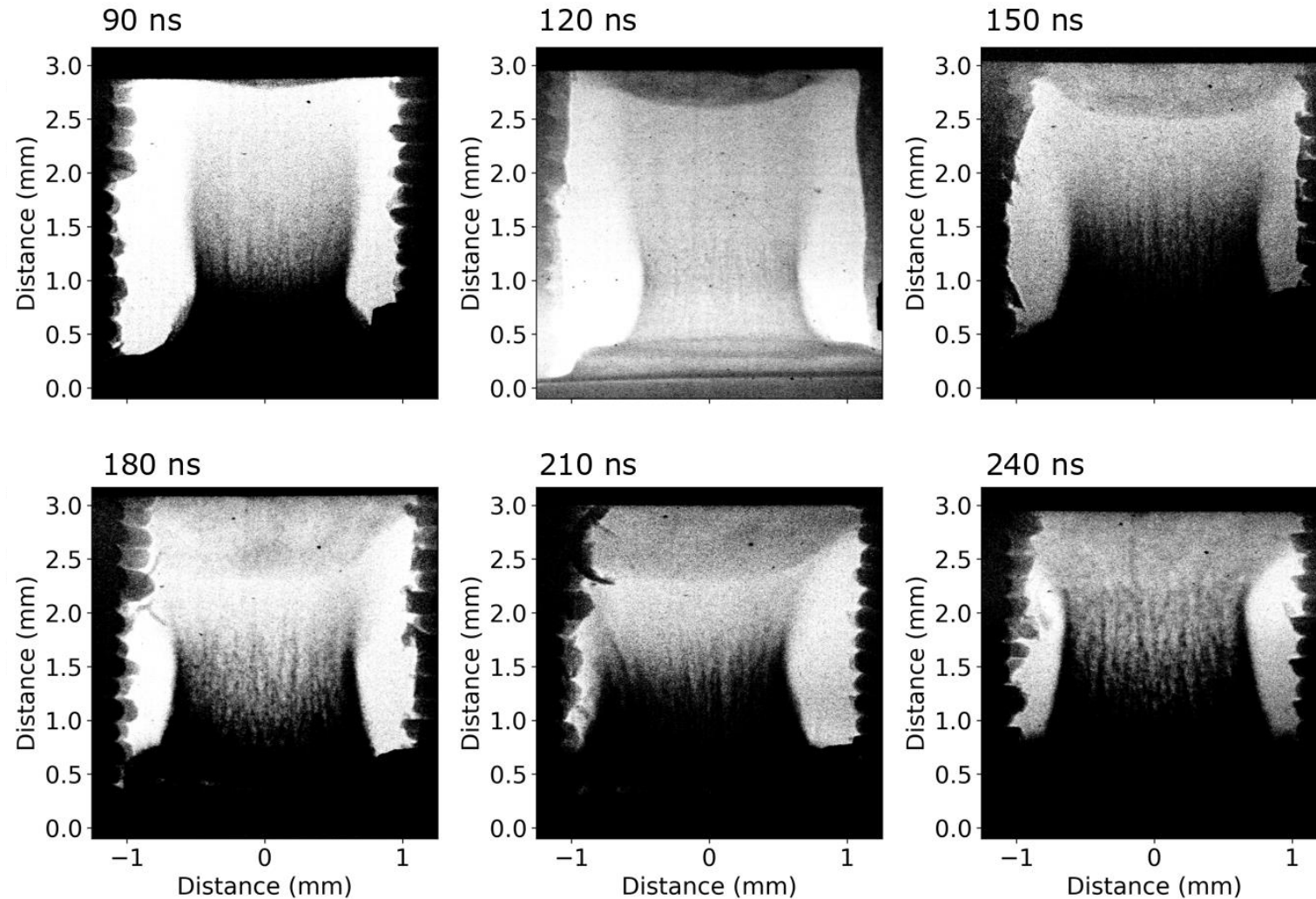
1D streaked

The B-field collimates the flow



The width of the plasma flow is decreased when the magnetic field is imposed due to the Lorentz force. The difference in the width of the jet is seen from 75 ns onwards (left). The subsequent increase in density of the incoming flow leads to a higher temperature reverse shock, as seen on the SOP (right).

X-ray radiography results

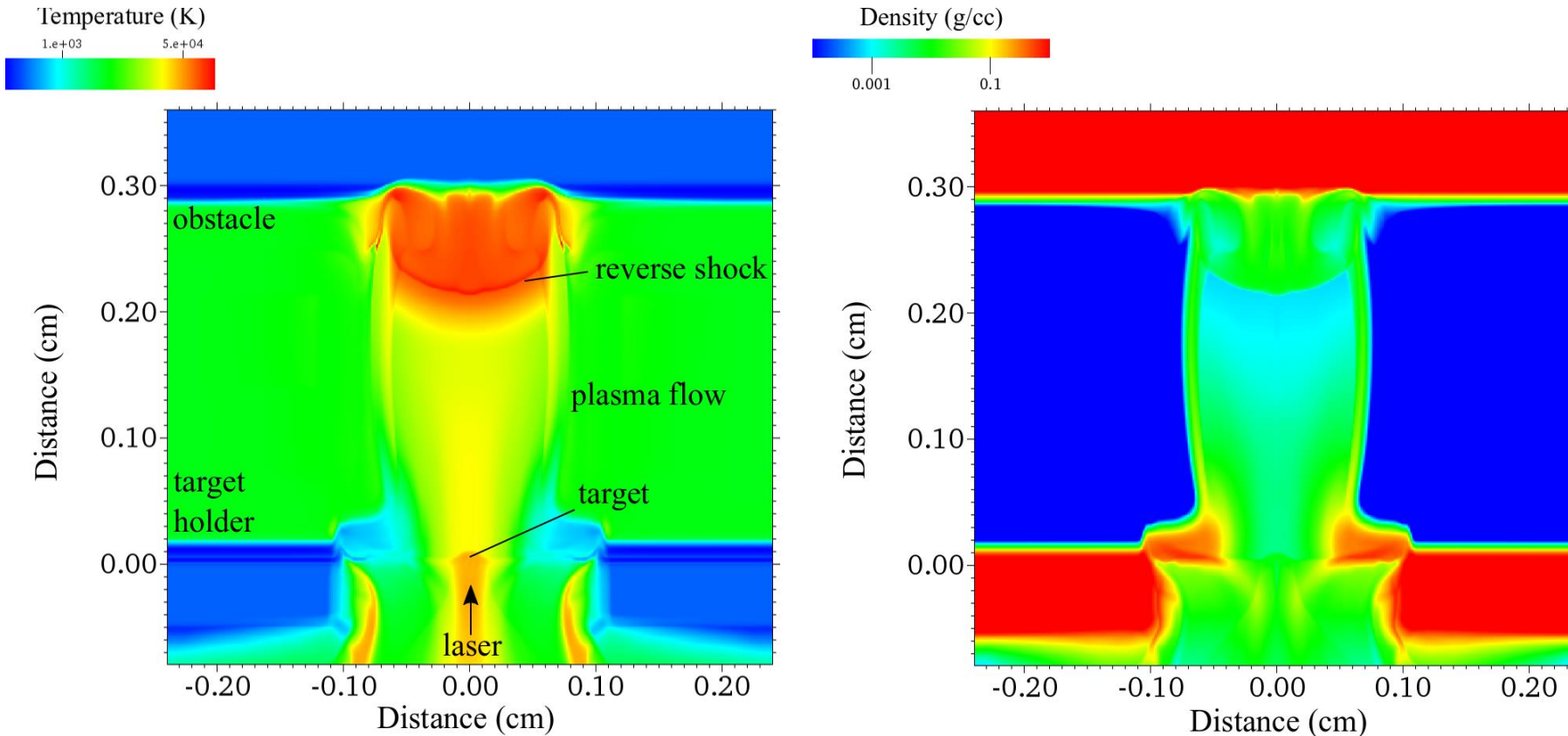


X-ray backlighter using ps driven titanium K-alpha radiation.

According to scaling laws, the reverse shock position in the laboratory should be between **1000 μm** and **450 μm** depending on the radiation model.

In our experiment, we measure **800 + 150 μm** .

MHD simulations with FLASH



Simulations performed with the MHD code, FLASH (developed at the University of Chicago).

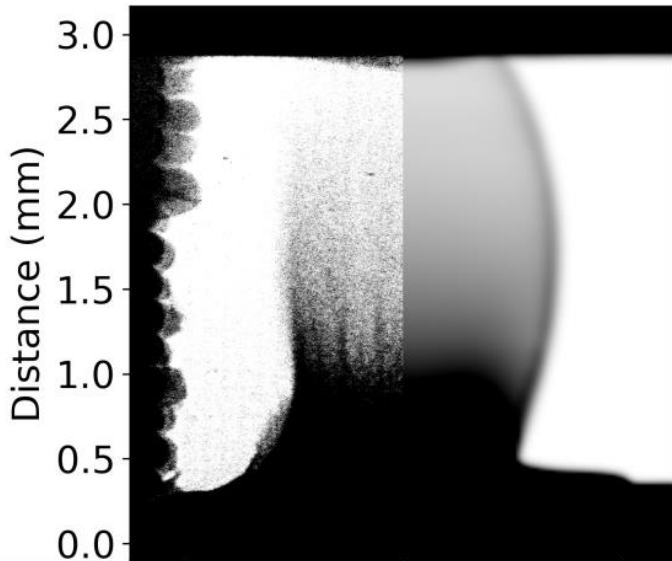
Non-ideal MHD, 2D, SESAME equation of state, radiation transfer solved in the multi-group diffusion. Simulation resolution of 5 microns

Temperature (left) and density (right) maps 150 ns after the laser drive.

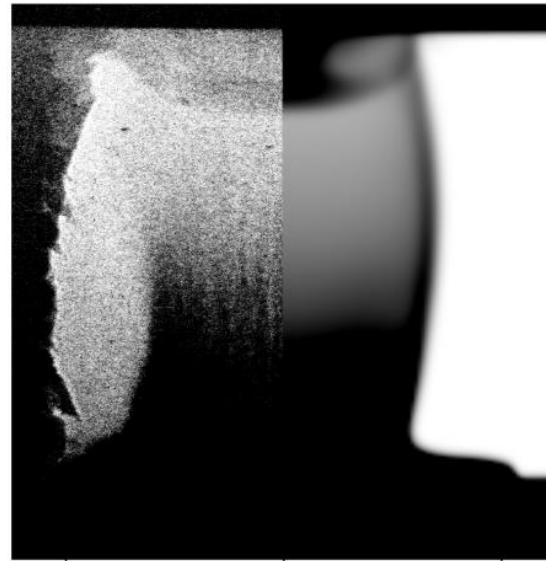
Simulations vs experimental data



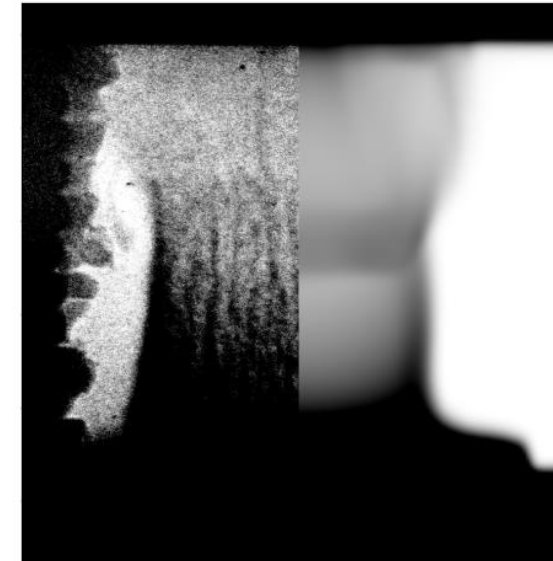
90 ns



150 ns



240 ns

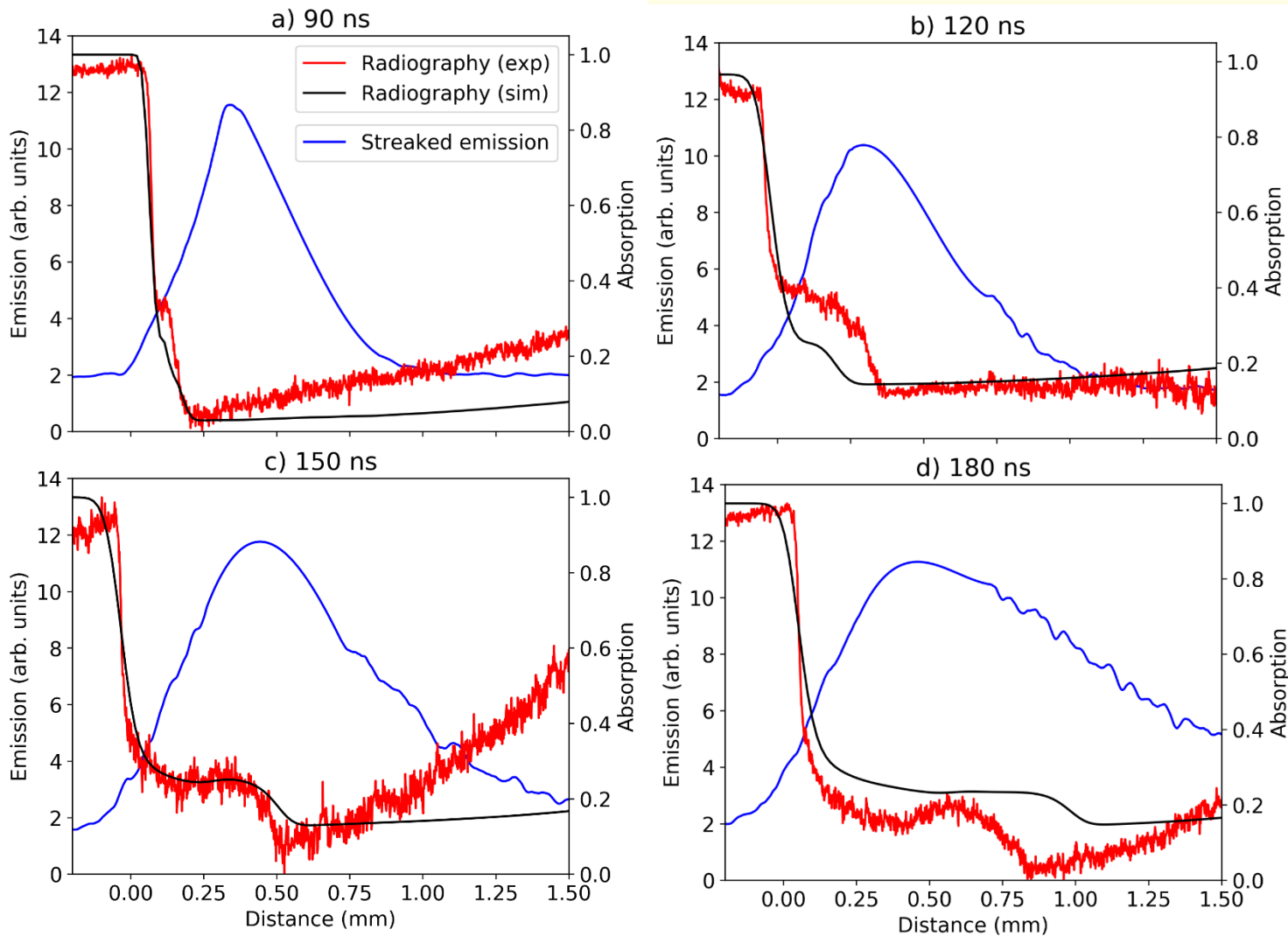


(left)
Experimental
data

(right)
Synthetic
radiography

The reverse shock does not stagnate in simulations. No mass is ejected transverse to the column or absorbed by the obstacle hence there is no mechanism to decelerate the shock on these timescales.

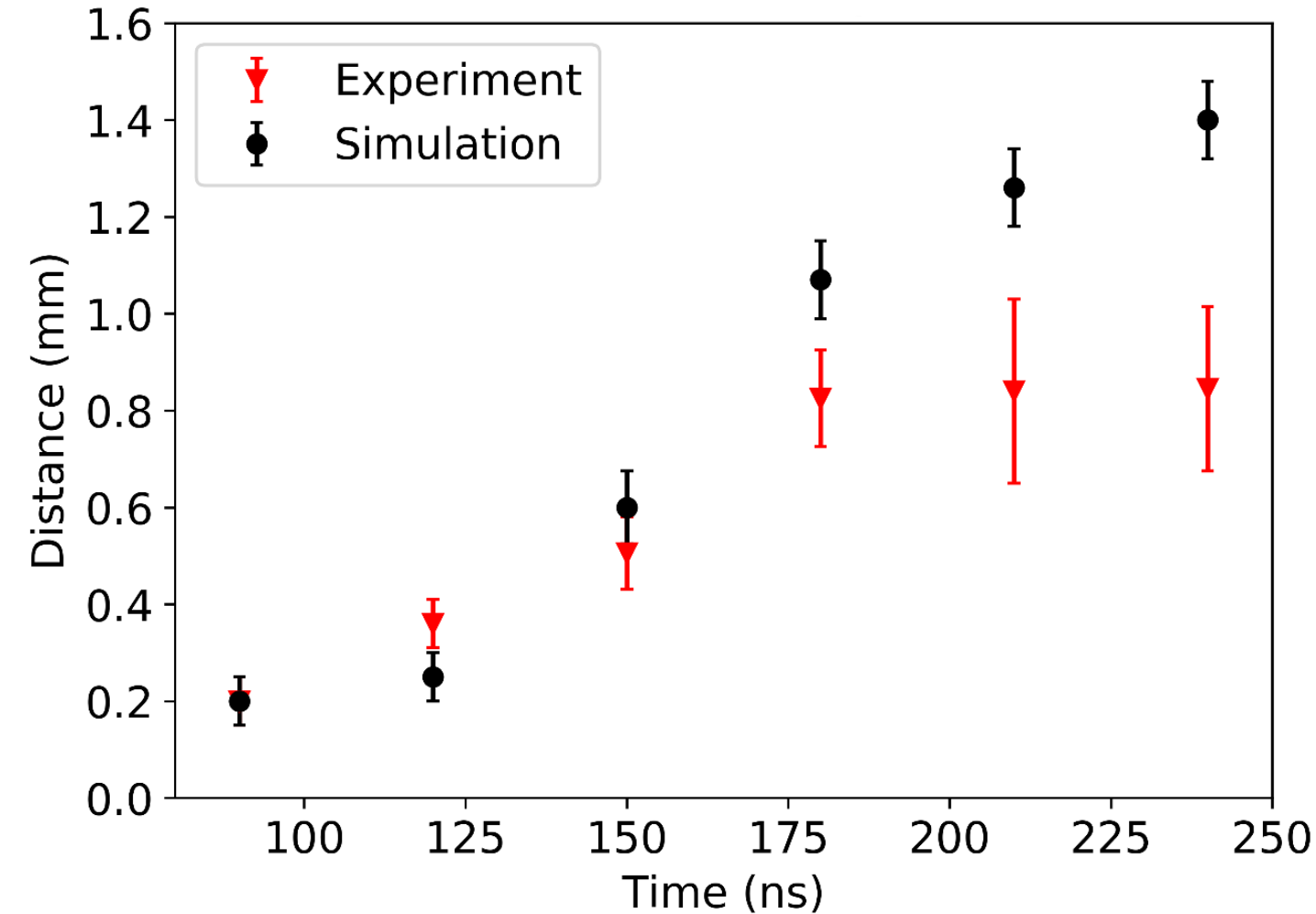
Evidence of a rarefaction wave



A hollow region between the obstacle and the shock front travelling away from the obstacle is observed.

Typical of a rarefaction wave, caused by the lateral mass ejection in the collision region.

Limitations of simulations



A hollow region between the obstacle and the shock front travelling away from the obstacle is observed.

Typical of a rarefaction wave, caused by the lateral mass ejection in the collision region.

Simulations currently unable to adequately treat transport across magnetic field lines in this scenario.

More conclusions and caveats



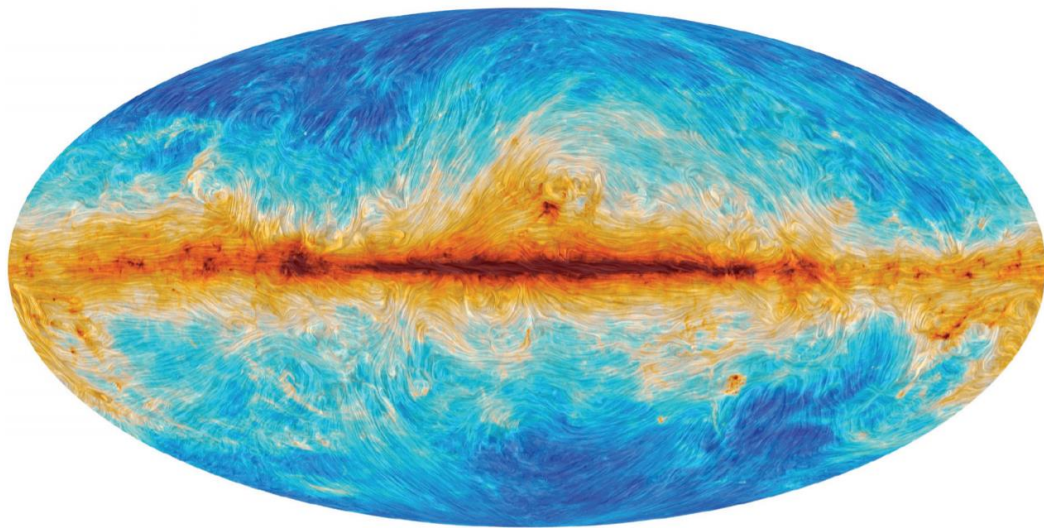
- According to scaling laws, the reverse shock position in the laboratory should be between **1000 μm** and **450 μm** depending on the radiation model.
 - In our experiment, we measure **800 \pm 150 μm** .
 - The experiment is well scaled to intermediate polars in terms of the magnetic pressure and the Reynolds number, *but not in terms of the radiation number*. Higher flow velocities are required in order for a direct comparison to be made.
 - At higher magnetic field strengths, can the flow be fully constrained by the B-field or do models need to take this mass loss into account? Does FLASH underestimate diffusivity?
 - Can we answer questions related to QPOs?
-

Talk outline

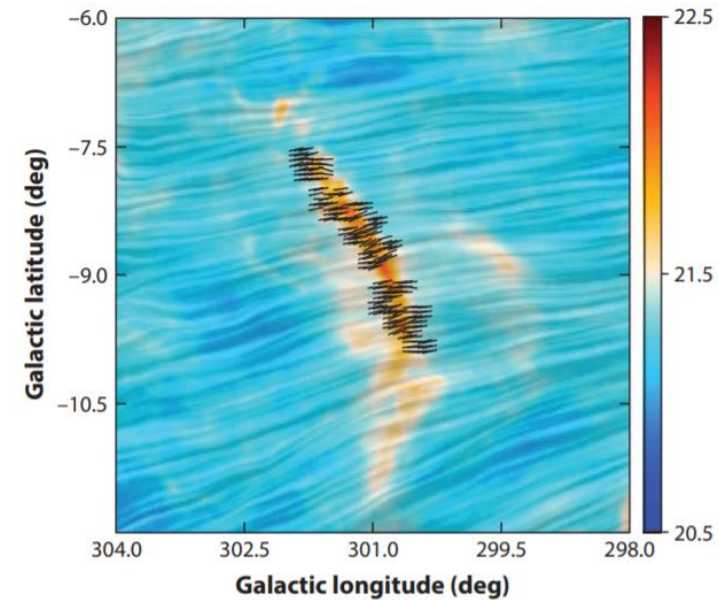
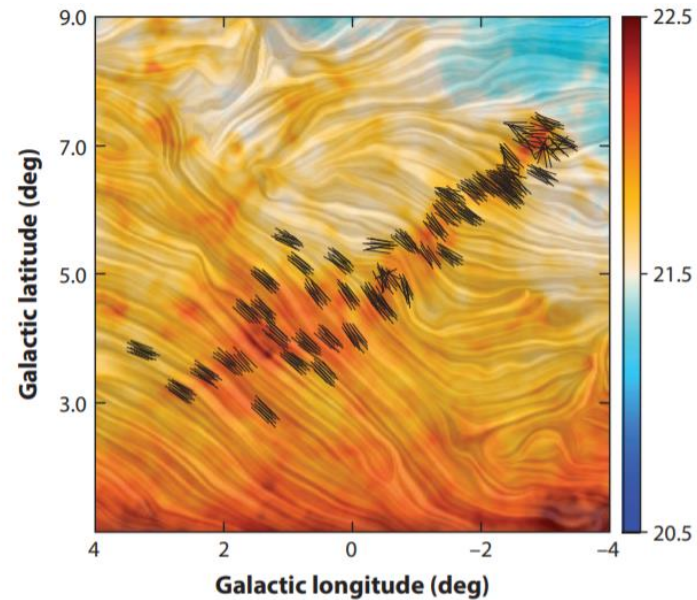


- What is laboratory astrophysics?
 - Magnetized accretion columns – POLAR project
 - **Hydromagnetic shocks and supernova remnants**
-

Celestial magnetic fields

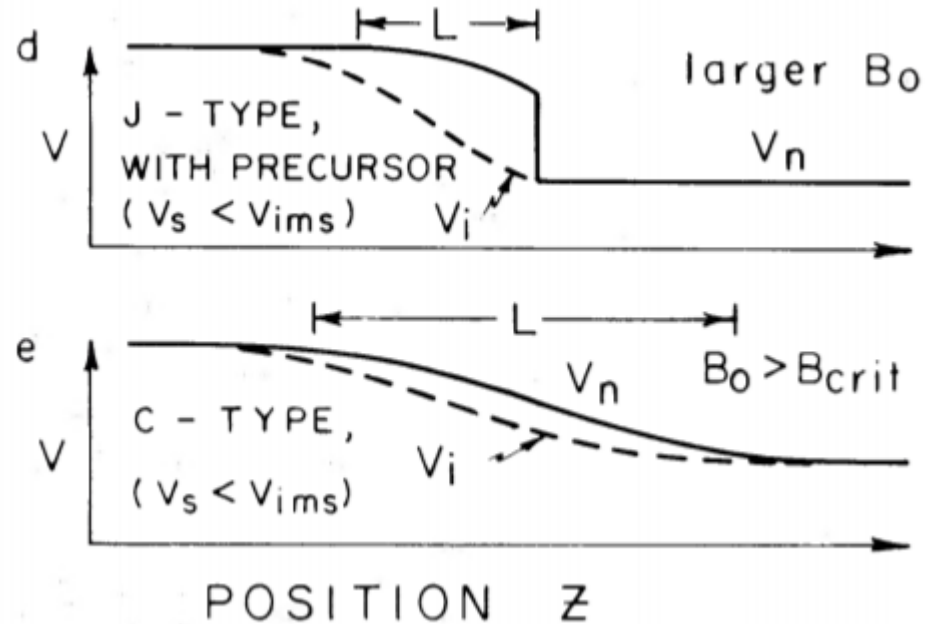
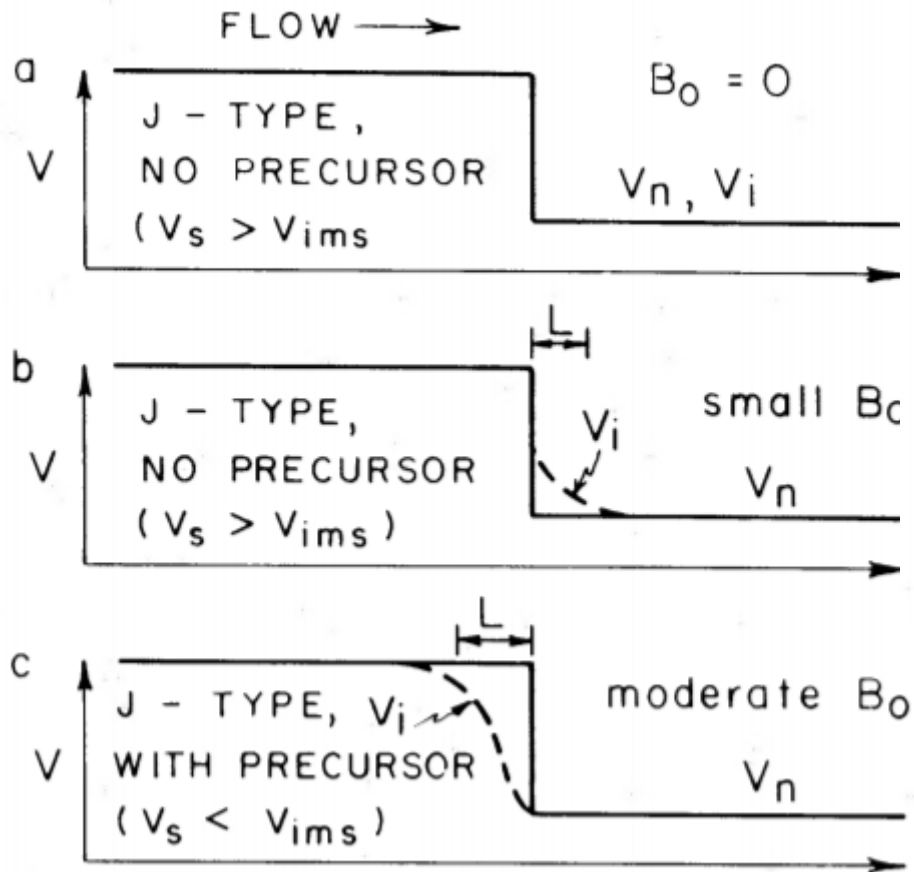


All-sky map of polarized thermal dust emission observed at 353 GHz by Planck showing the orientation of B_{\perp} as the flow pattern. Planck Collab. et al. (2016a) © ESO.



Magnetic field orientations in the Pipe and Musca molecular clouds inferred from the polarized thermal dust emission by Planck images (same color scheme as Figure 1) and starlight polarization (black bars). Soler et al. (2016) © ESO

Theory of hydromagnetic shocks



Draine et al. ApJ 241:1021-1038, 1980

When the magnetic field is increased such that the magnetosonic speed becomes larger than the shock speed, ions are able to travel upstream in front of the shock, leading to the formation of a magnetic precursor.

Observations of hydromagnetic shocks



THE ASTROPHYSICAL JOURNAL LETTERS, 881:L42 (6pp), 2019 August 20
© 2019. The American Astronomical Society. All rights reserved.

<https://doi.org/10.3847/2041-8213/ab38c5>



Interstellar Plunging Waves: ALMA Resolves the Physical Structure of Nonstationary MHD Shocks

Giuliana Cosentino^{1,2}, Izaskun Jiménez-Serra^{3,4}, Paola Caselli⁵, Jonathan D. Henshaw⁶, Ashley T. Barnes⁷, Jonathan C. Tan^{8,9}, Serena Viti¹, Francesco Fontani¹⁰, and Benjamin Wu¹¹

¹ Department of Physics and Astronomy, University College London, Gower Street, London WC1E6BT, UK; giuliana.cosentino.15@ucl.ac.uk

² European Southern Observatory, Karl-Schwarzschild-Strasse 2, D-85748 Garching, Germany

³ Departamento de Astrofísica, Centro de Astrobiología, E-28850 Torrejón de Ardoz, Madrid, Spain

⁴ School of Physics & Astronomy, Queen Mary University of London, Mile End Road, London E1 4NS, UK

⁵ Max-Planck Institute for Extraterrestrial Physics, Gießenbachstrasse 2, D-85748 Garching, Germany

⁶ Max-Planck Institute for Astronomy, Königstuhl 17, D-69117 Heidelberg, Germany

⁷ Argelander-Institut für Astronomie Auf dem Hügel 71, D-53121 Bonn, Germany

⁸ Space, Earth and Environment Department, Chalmers University of Technology, Chalmersplatsen 4, SE-41296 Göteborg, Sweden

⁹ Department of Astronomy, University of Virginia, Charlottesville, VA, USA

¹⁰ INAF-Osservatorio Astrofisico di Arcetri, Largo E. Fermi 2, I-50125 Firenze, Italy

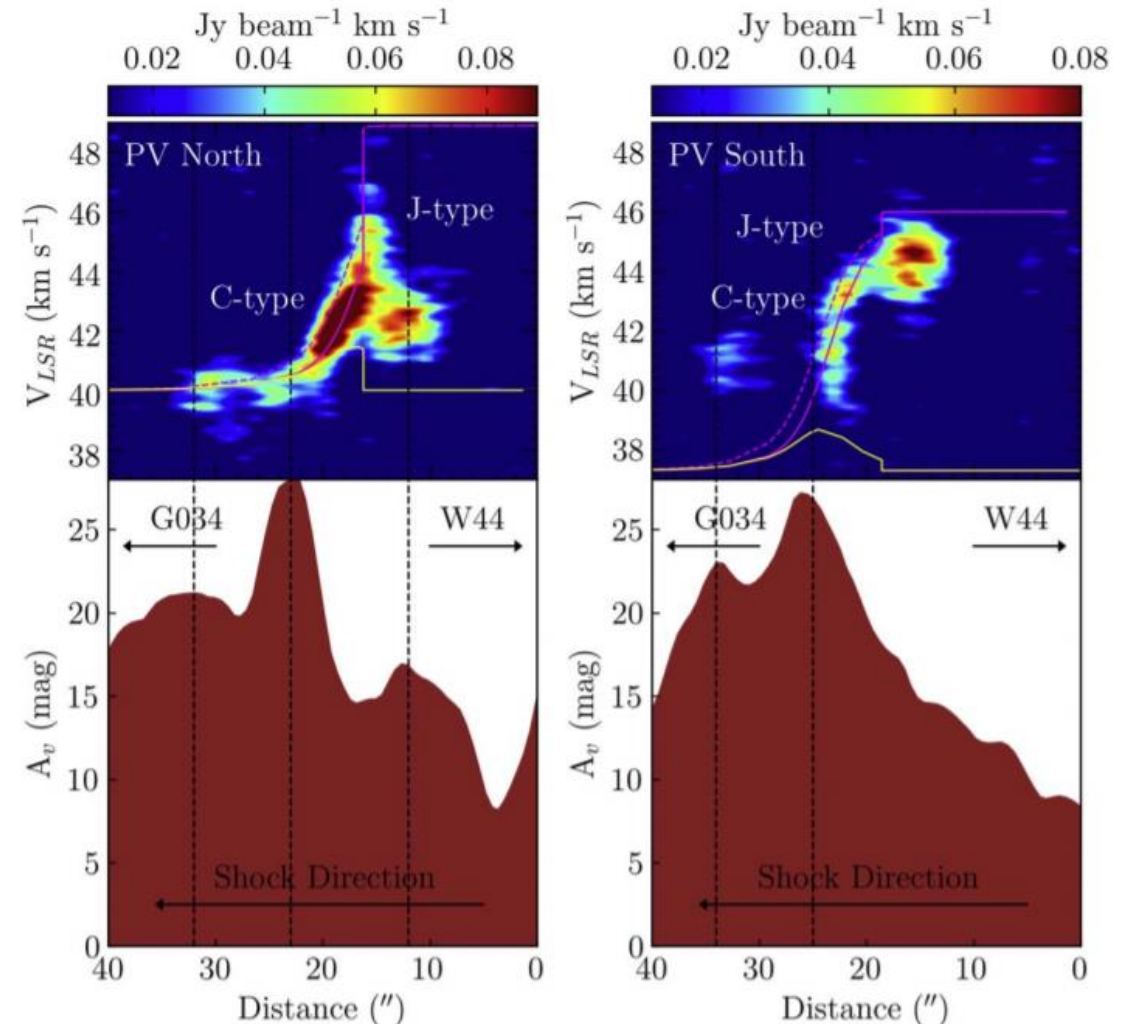
¹¹ National Astronomical Observatory of Japan, Yubinbango 181-8588 Tokio, Mitaka, Osawa 2-21-1, Japan

Received 2019 June 24; revised 2019 August 1; accepted 2019 August 6; published 2019 August 21

Abstract

Magnetohydrodynamic (MHD) shocks are violent events that inject large amounts of energy in the interstellar medium dramatically modifying its physical properties and chemical composition. Indirect evidence for the presence of such shocks has been reported from the especial chemistry detected toward a variety of astrophysical shocked environments. However, the internal physical structure of these shocks remains unresolved since their expected spatial scales are too small to be measured with current instrumentation. Here we report the first detection of a fully spatially resolved, MHD shock toward the infrared dark cloud (IRDC) G034.77-00.55. The shock, probed by silicon monoxide (SiO) and observed with the Atacama Large Millimeter/submillimeter Array (ALMA), is associated with the collision between the dense molecular gas of the cloud and a molecular gas flow pushed toward the IRDC by the nearby supernova remnant (SNR) W44. The interaction is occurring on subparsec spatial scales thanks to the enhanced magnetic field of the SNR, making the dissipation region of the MHD shock large enough to be resolved with ALMA. Our observations suggest that molecular flow–flow collisions can be triggered by stellar feedback, inducing shocked molecular gas densities compatible with those required for massive star formation.

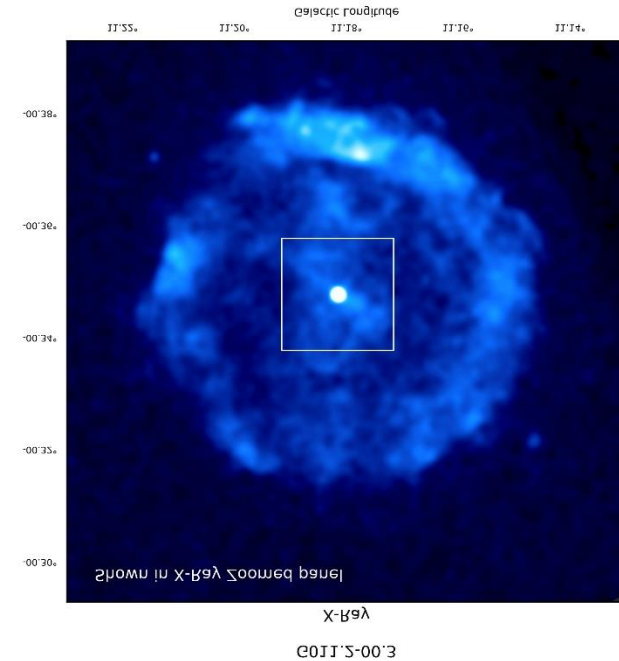
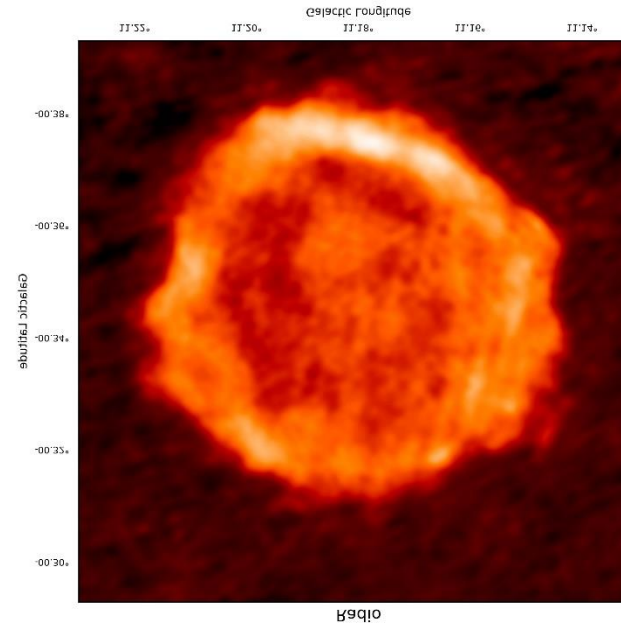
Key words: ISM: clouds (G034.77-00.55) – ISM: molecules – ISM: supernova remnants (W44) – shock waves



Supernova remnants and Sedov-Taylor



- Self-similar solution independent of scale.
- Assumes point like energy source.
- Isotropic expansion
- Ram pressure of blast wave dominates ambient pressure.
- Radiative effects are negligible.
- Shown to work in astrophysical and terrestrial systems



J. L. West et al. A&A 587, A148 (2016)

$$r \propto (E_0/\rho_0)^{1/5} t^{2/5}$$

Barrel-shaped SNRs (G296.5+10.0)

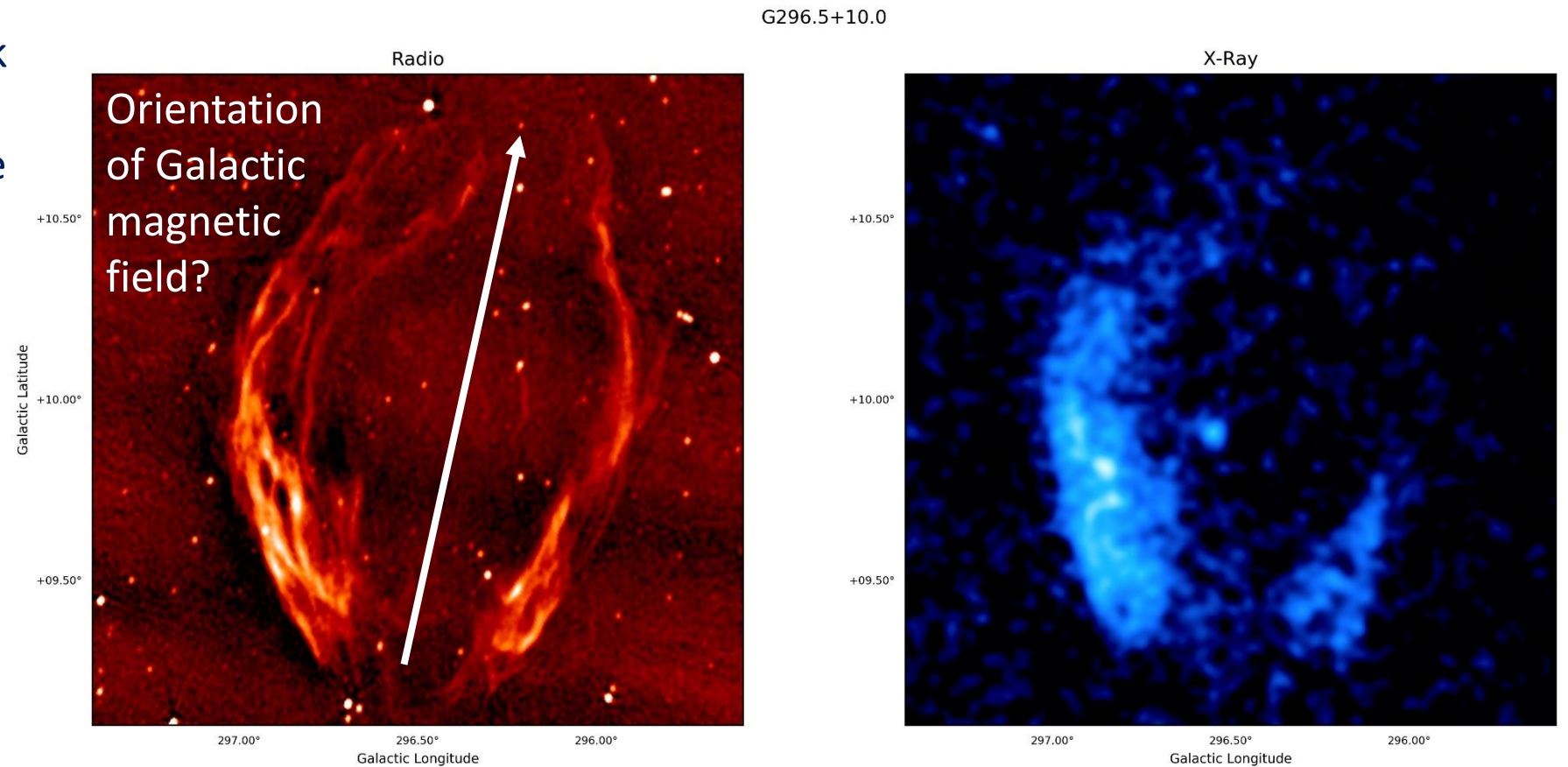


Observations suggest a link between barrel-shaped / axisymmetric SNRs and the galactic magnetic field.

J. L. West et al. A&A 587, A148 (2016)

Or evidence for a magnetized progenitor wind

Harvey-Smith, L., et al. ApJ 712.2 (2010): 1157



Experimental aims and scaling laws



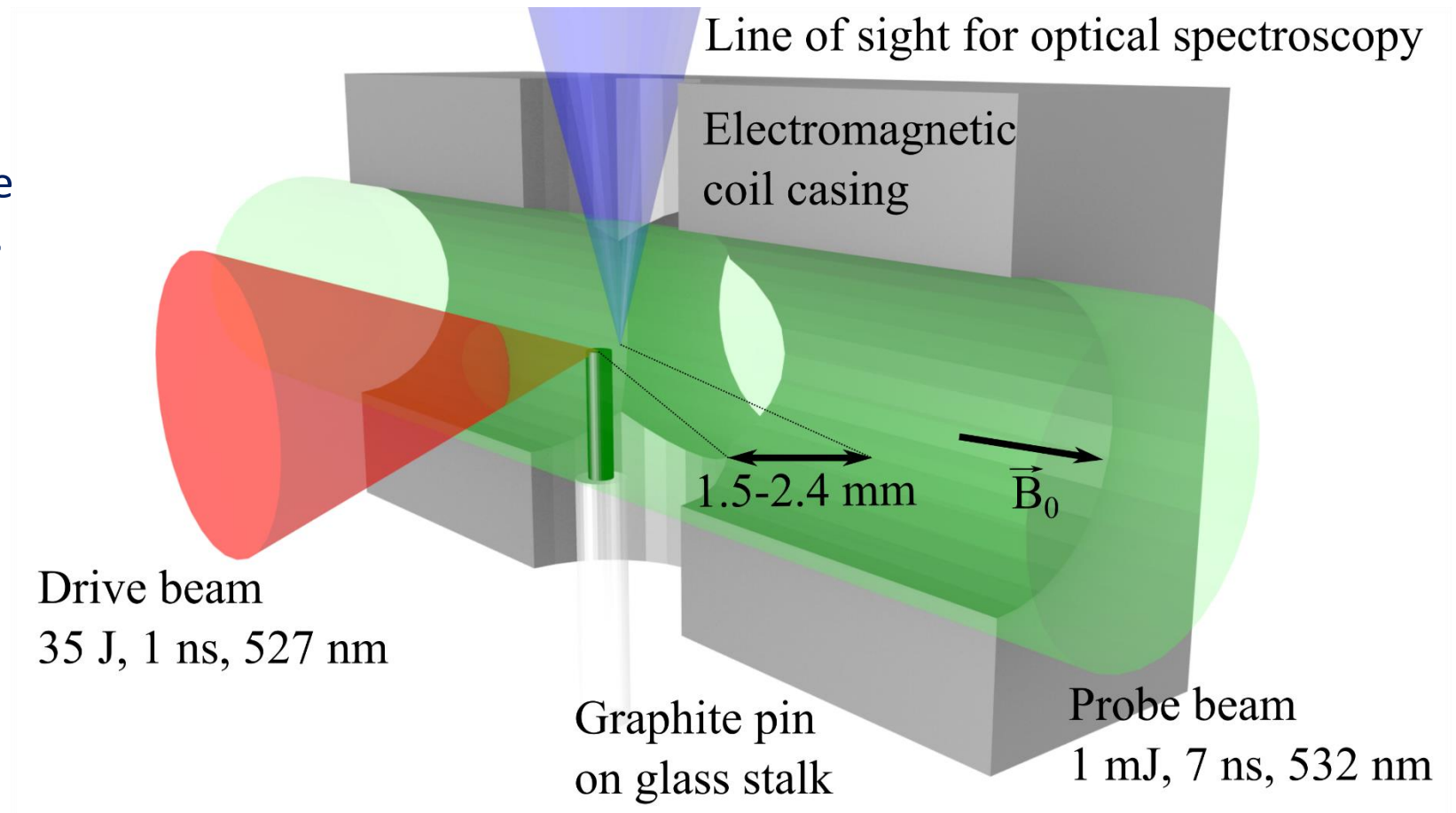
- Test hypothesis that uniform magnetic field causes barrel-shape blast wave
 - Create MHD shocks in controlled environment and test theory.
 1. *Magnetic Reynolds number $\gg 1$ in both systems (ratio of magnetic advection to diffusion)*
 2. *Plasma beta similar in both systems (ratio of ram pressure to magnetic pressure)*
-

Creating a blast wave in the lab



P. Mabey et al. ApJ Submitted

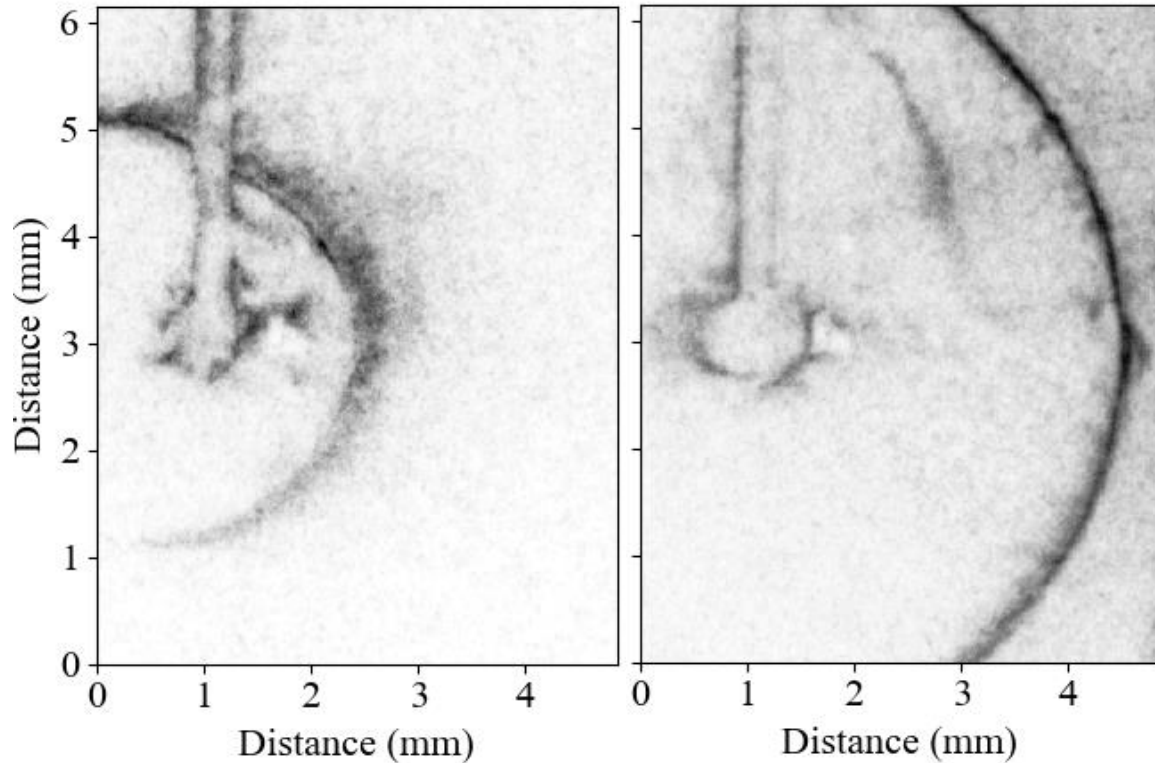
- The drive laser irradiates a carbon pin target.
- This causes a blast wave to be generated in the ambient gas inside the chamber.
- Optical diagnostics are employed in the two perpendicular axes.
- The entire experiment is housed in a coil in order to generate the magnetic field



Blast wave propagation (schlieren)



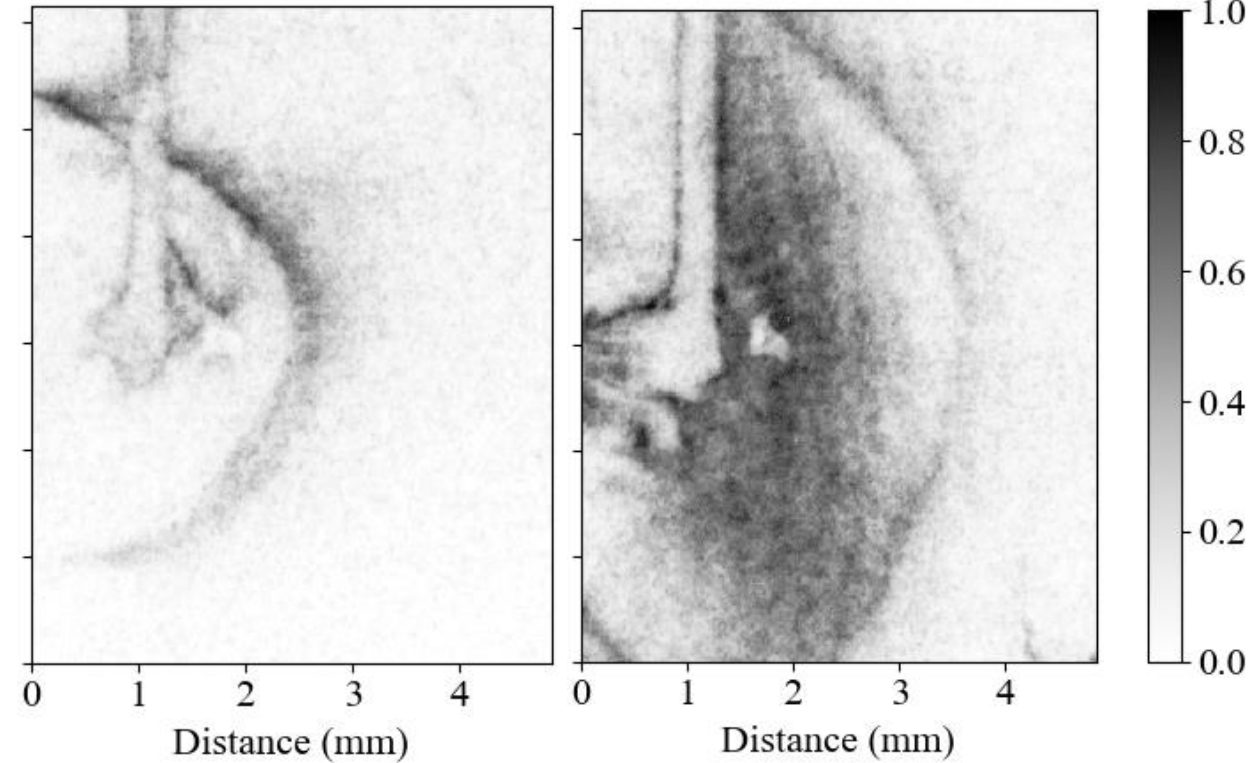
Without magnetic field



20 ns

80 ns

10.2 T



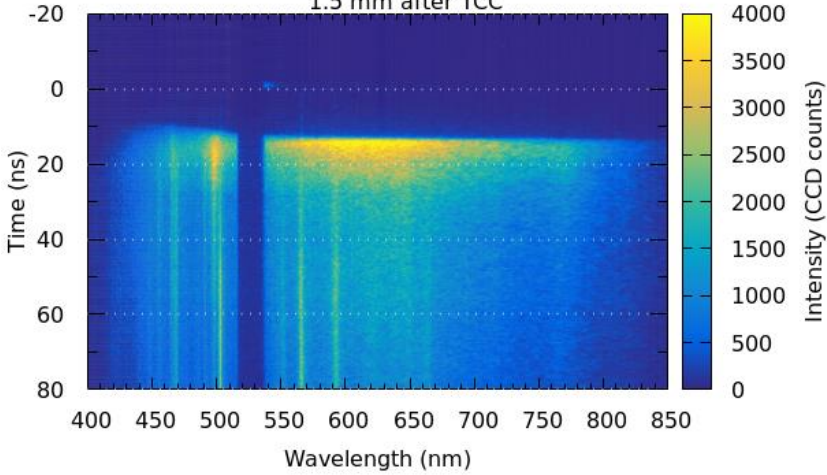
20 ns

80 ns

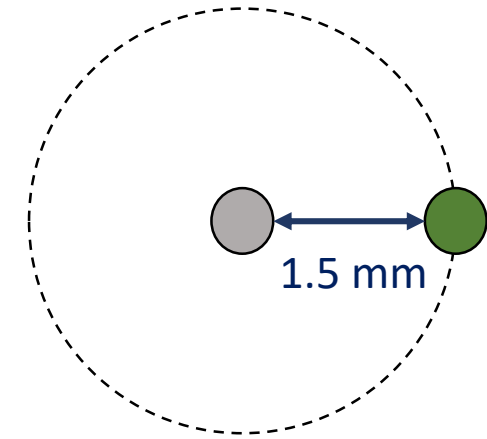
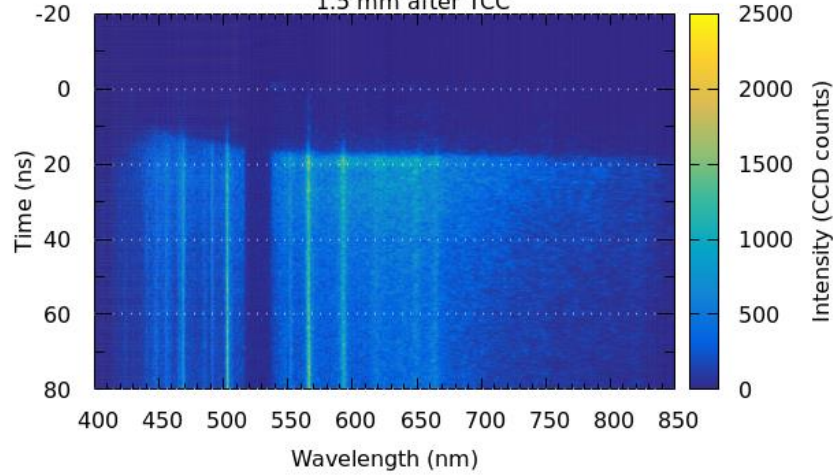
Blast wave propagation (spectroscopy)



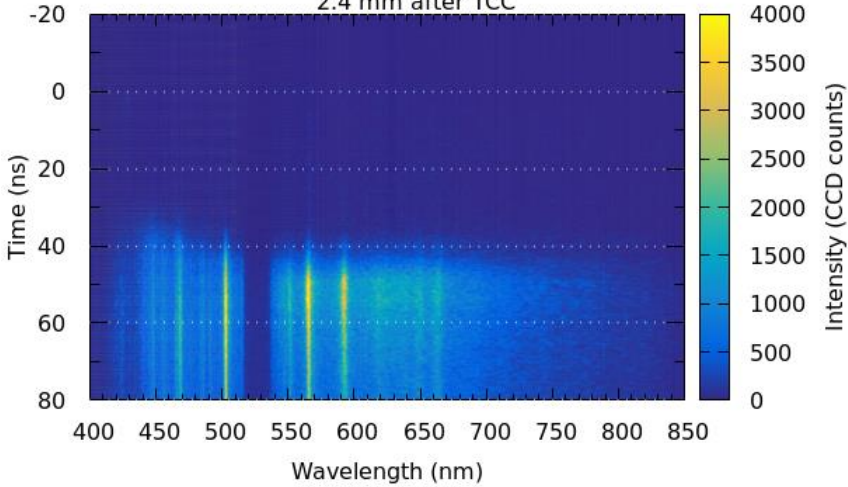
Shot 78 ; w/o B-field ; minimum focal spot, w BG filter ; 44 J
1.5 mm after TCC



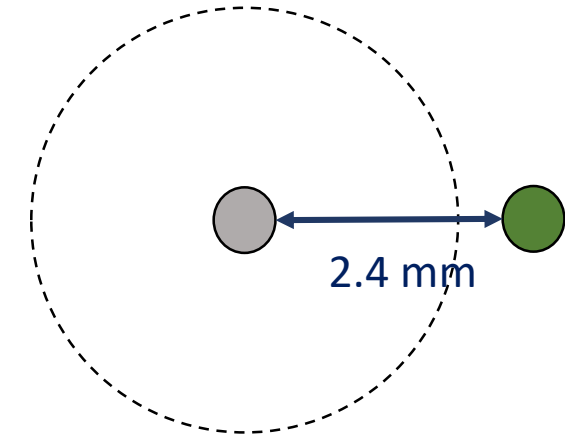
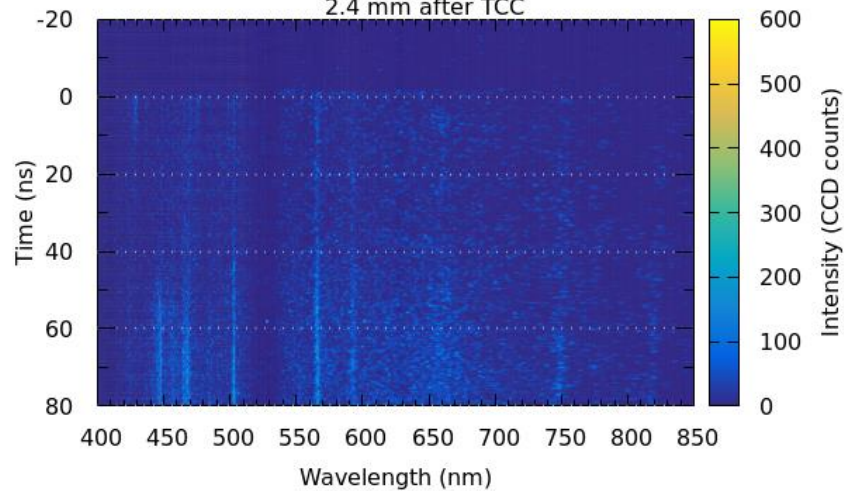
Shot 74 ; w B-field perpendicular, 10 T; minimum focal spot, w BG filter ; 38 J
1.5 mm after TCC



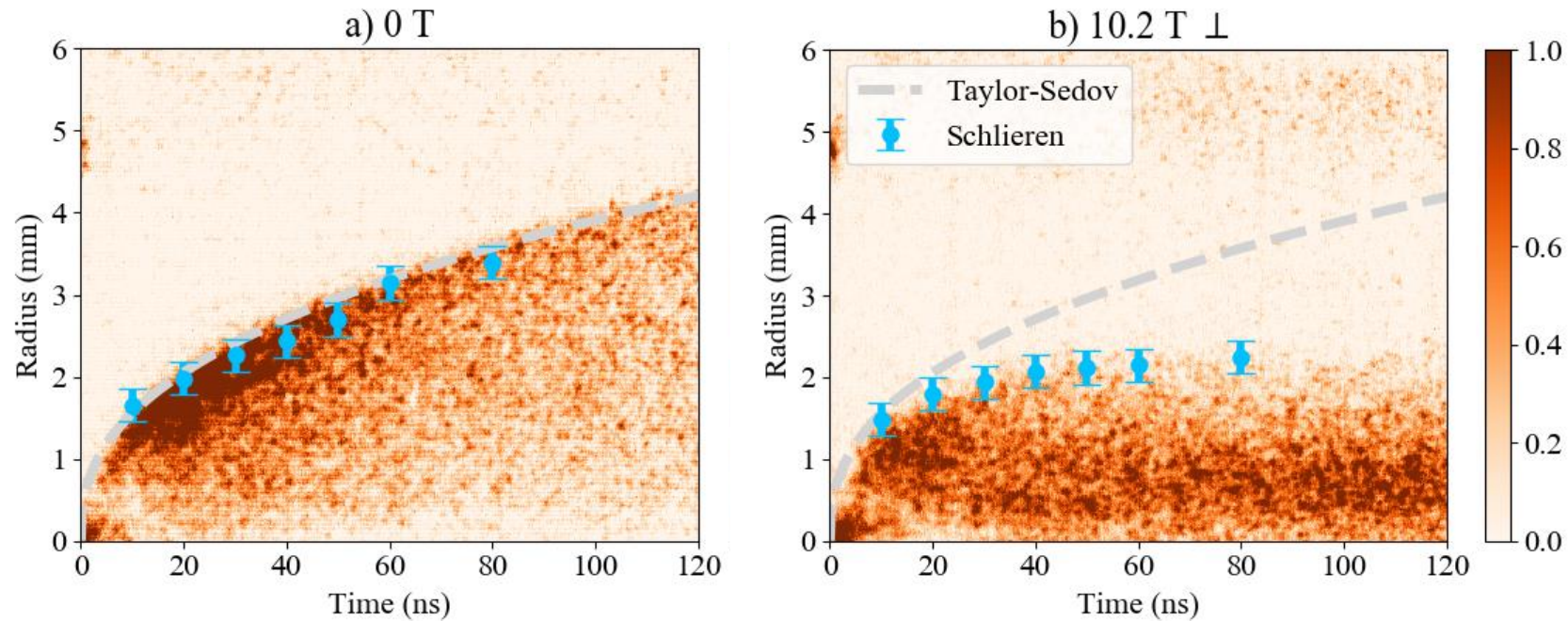
Shot 69 ; w/o B-field; minimum focal spot, w BG filter ; 43 J
2.4 mm after TCC



Shot 68 ; w B-field perpendicular, 10 T; minimum focal spot, w BG filter ; 44 J
2.4 mm after TCC

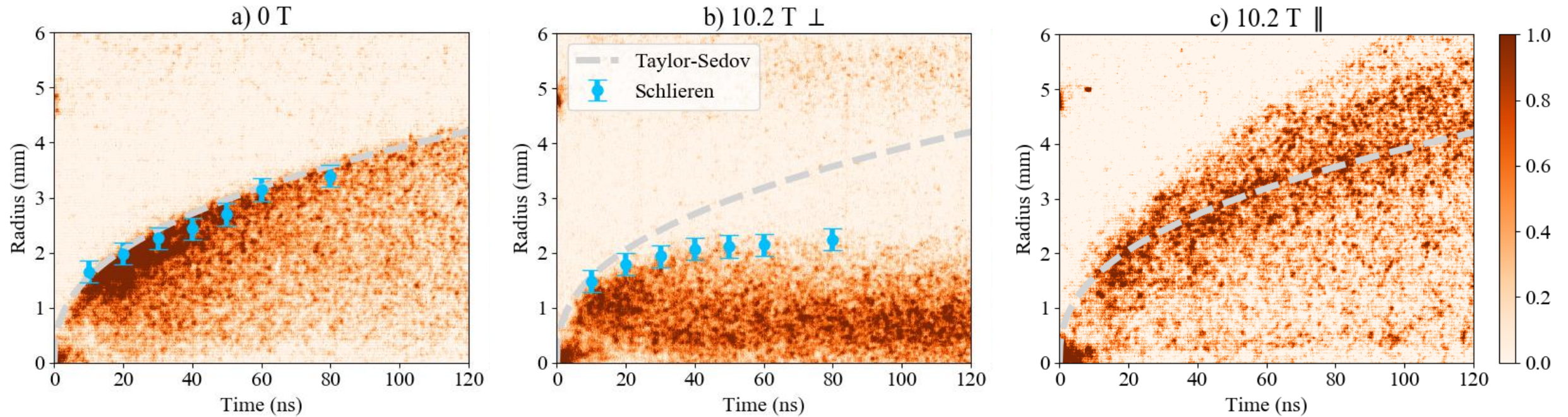


Deviation from TS regime



Blast wave decelerates *faster* than Taylor-Sedov *perpendicular* to magnetic field

Evidence of a barrel shape



Blast wave decelerates *slower* than Taylor-Sedov *parallel* to magnetic field

Barrel shaped blast wave



Without magnetic field

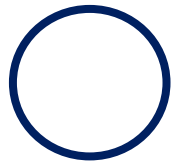
Magnetic field →



Barrel shaped blast wave



Without magnetic field



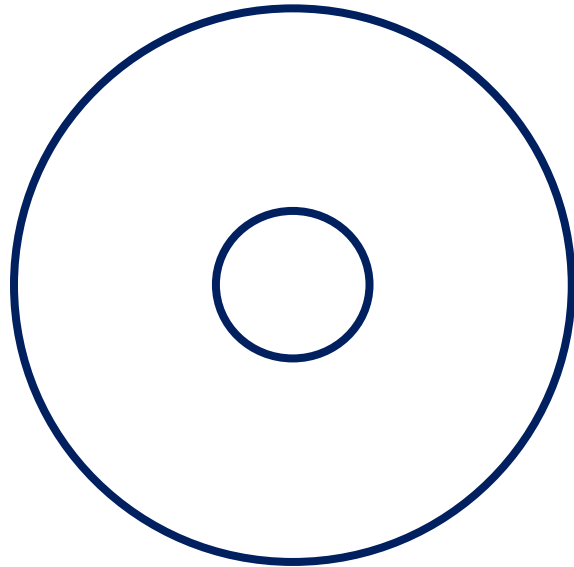
Magnetic field →



Barrel shaped blast wave



Without magnetic field



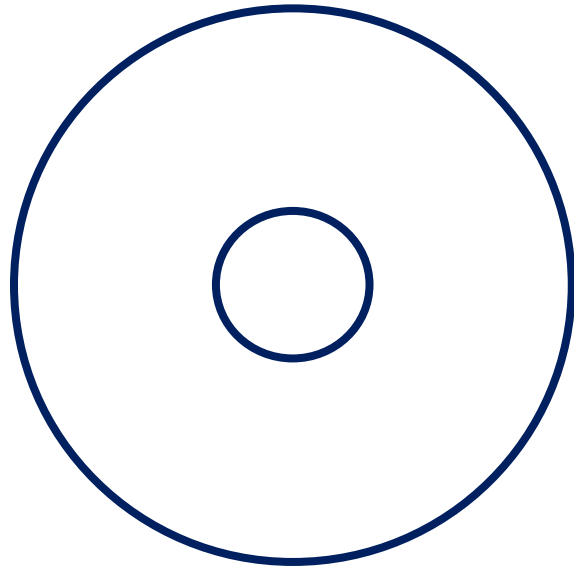
Magnetic field →



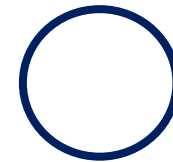
Barrel shaped blast wave



Without magnetic field



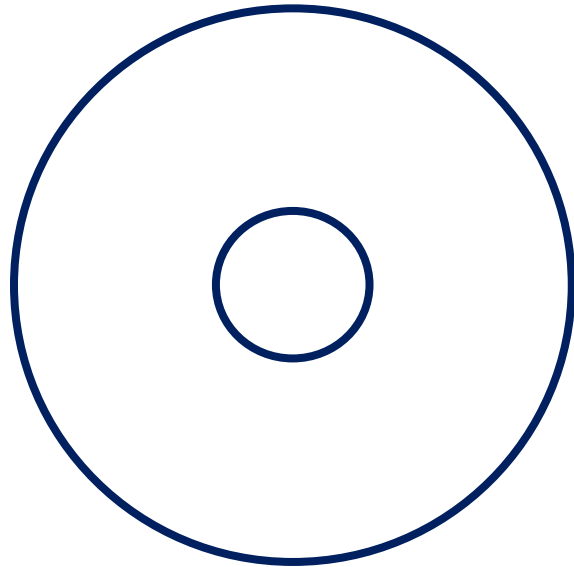
Magnetic field →



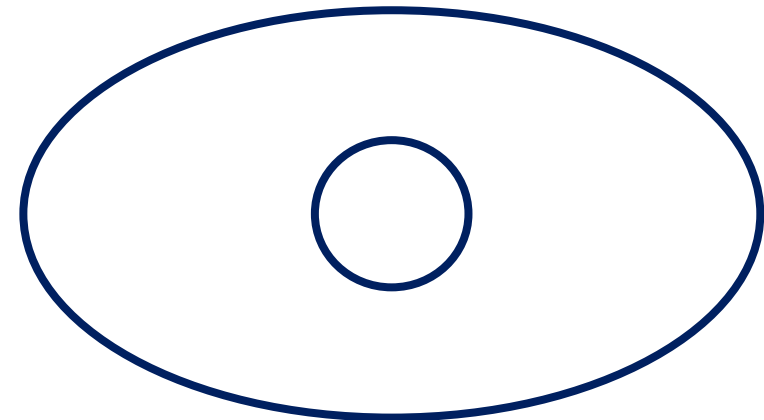
Barrel shaped blast wave



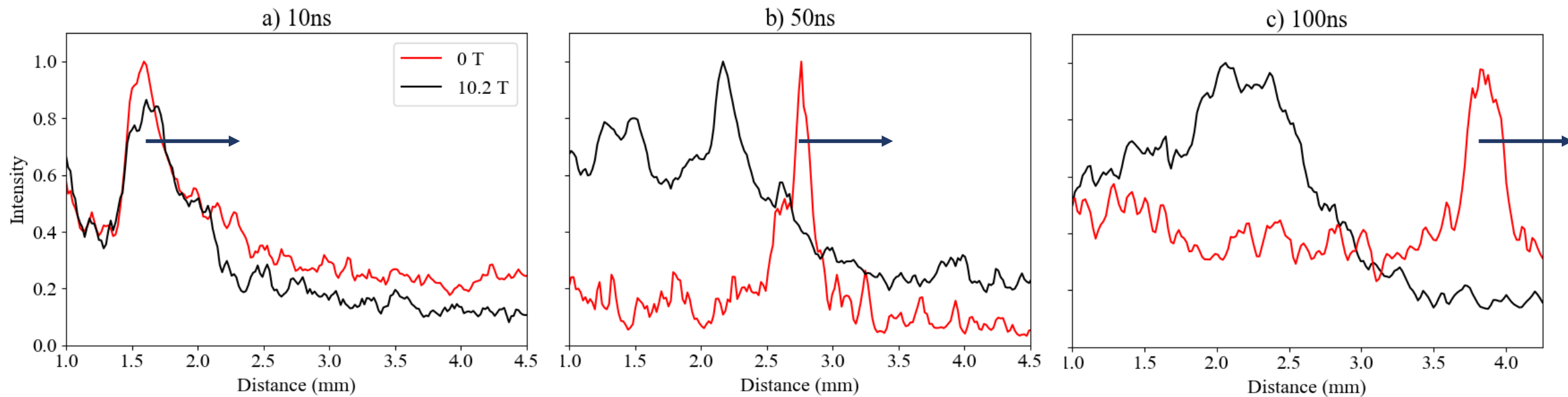
Without magnetic field



Magnetic field →



Increased width of BW shell (schlieren)

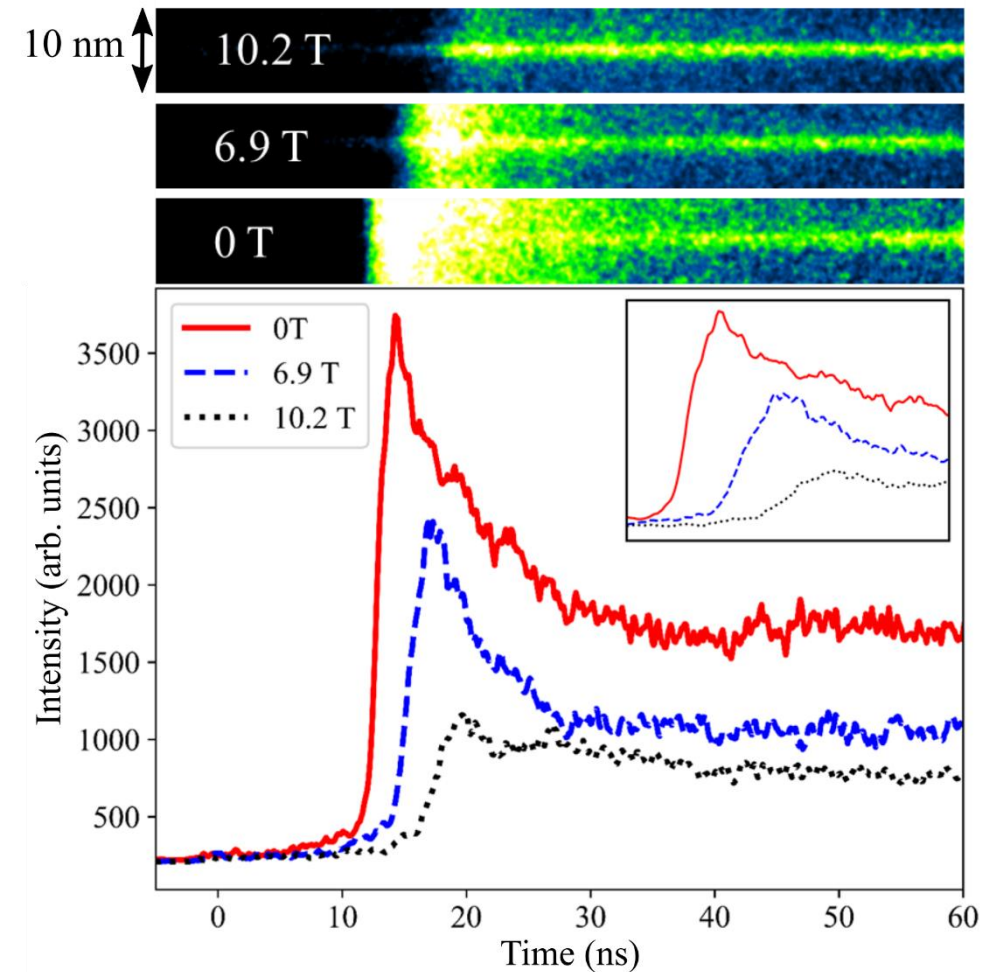
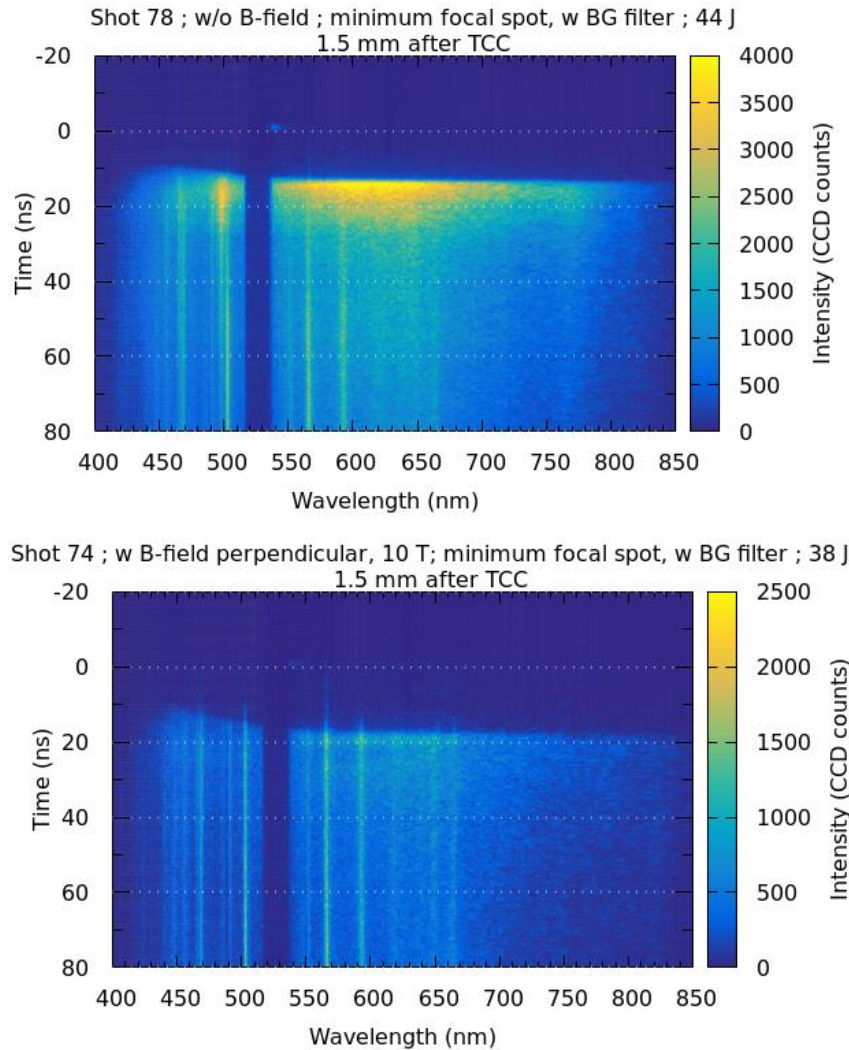


Width of blast wave with magnetic field (black) increases with time

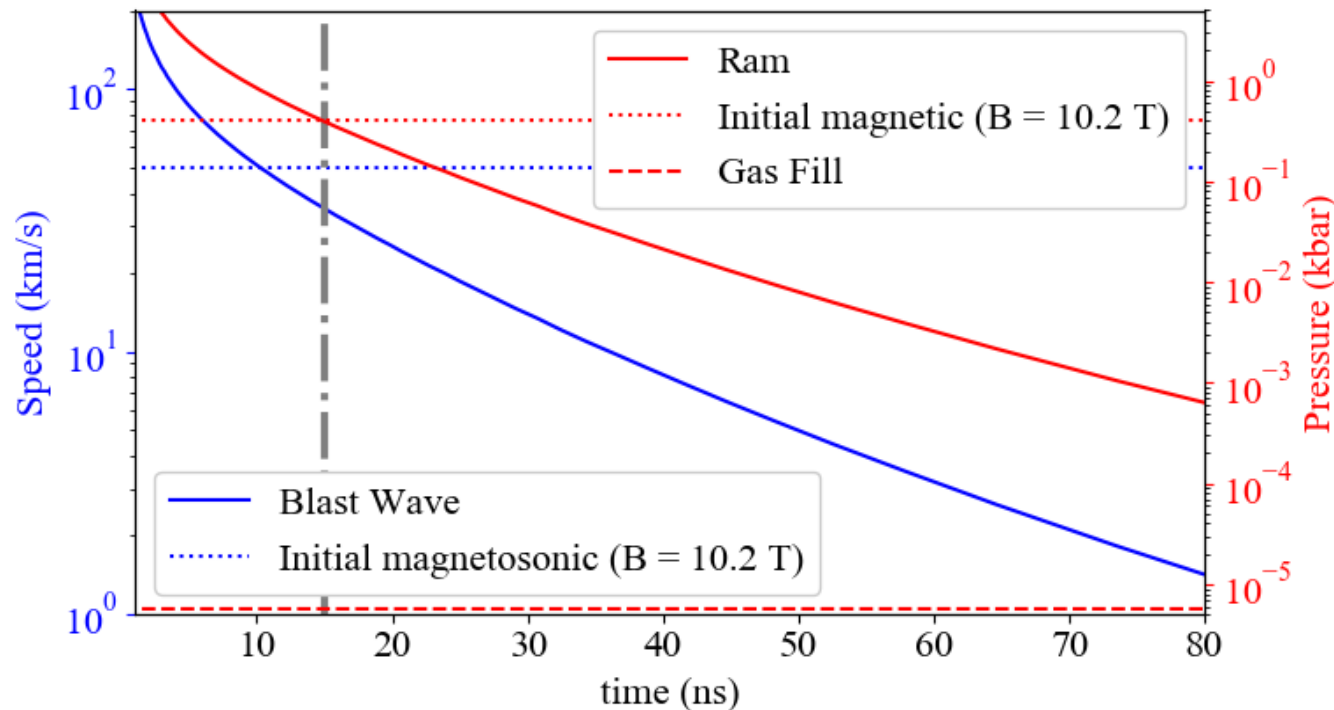
Increased width of BW shell (spectroscopy)



Increase in intensity of NII emission lines occurs more gradually with increasing magnetic field strength



Magnetic effects grow over time



- Speed of blast wave is high initially, $\beta \gg 1$, $v_s > v_{ms}$ magnetic effects are small.
- Blast wave slows down due to Taylor-Sedov law
- At some time later, $\beta \sim 1$ and $v_s \sim v_{ms}$ blast wave changes morphology and shell thickness
- Blast wave decelerates further when B is perpendicular, creating positive feedback loop

Determining the magnetic field



Flux conservation

$$B(\phi) = \frac{r^2}{r^2 - (r - d)^2} B_0 \sin(\phi)$$

Van der Laan, H. 1962, MNRAS, 124, 125

Magnetic field initially increases from 10.2 T to 24 T (radius dominates).

Then relaxes back down towards its initial value (shell width dominates).

Jump conditions

$$(\rho v^2 + P + B_{\perp}^2/2\mu_0)_1 - (\rho v^2 + P + B_{\perp}^2/2\mu_0)_0 = 0$$

Shu, F. H. 1991, The Physics of Astrophysics: Gas Dynamics, Vol. 2

Temperature and density measurements taken at single point corresponding to 50 ns.

B = 15 T

Two methods in agreement.

What does this mean for G296.5+10.0?



Age = 10,000 years

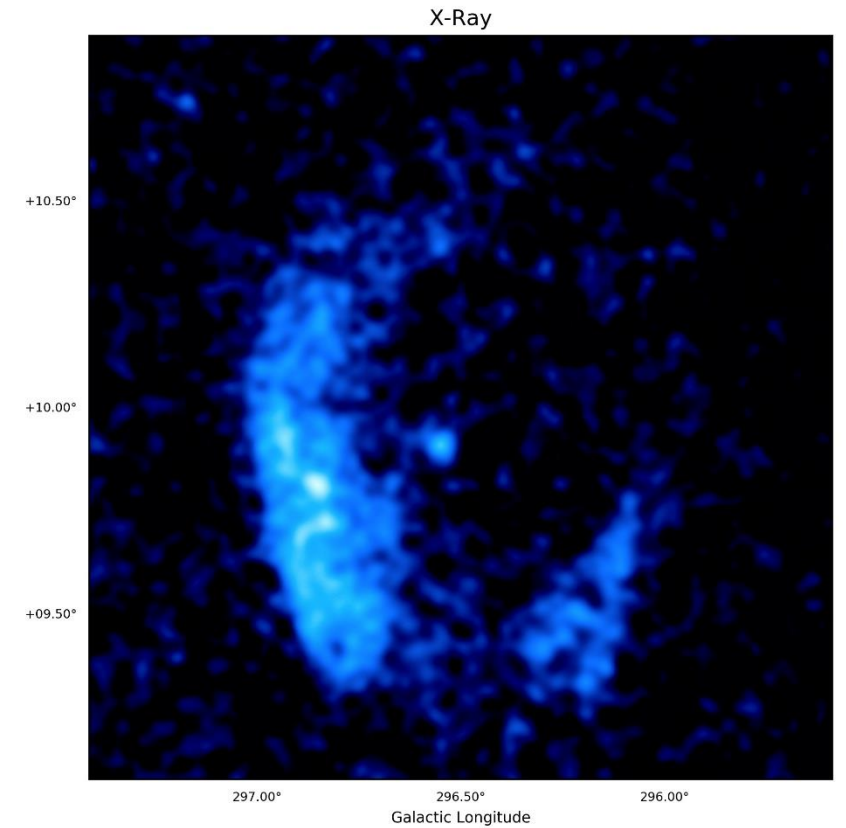
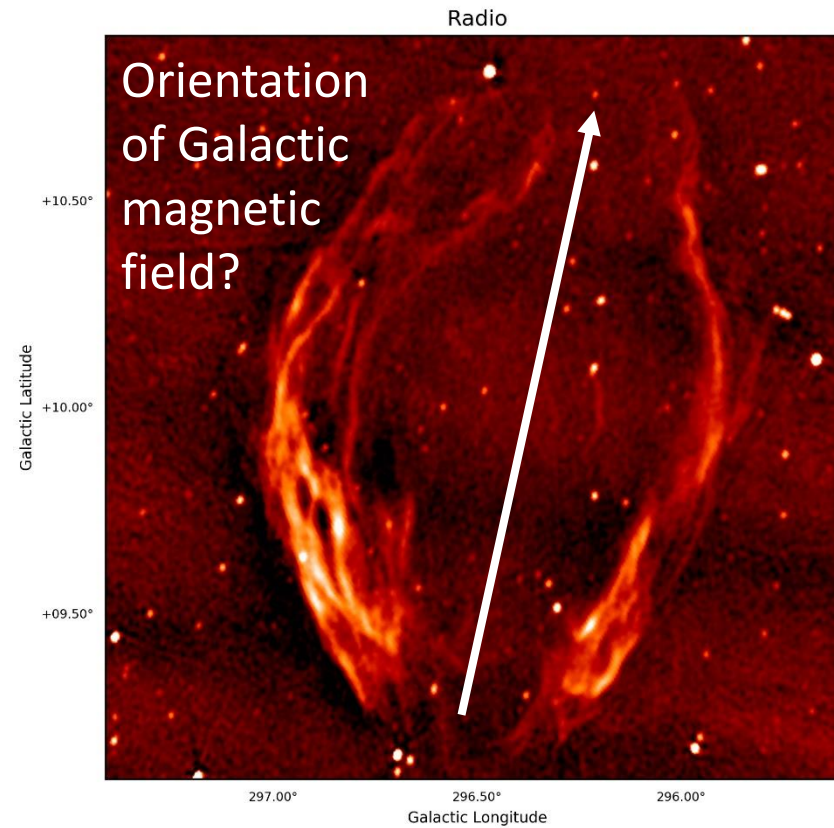
Explosion energy = 10^{51} erg

Magnetic field = $50 \mu\text{G}$

Density = 0.1 cm^{-3}

$\beta = 5$

G296.5+10.0

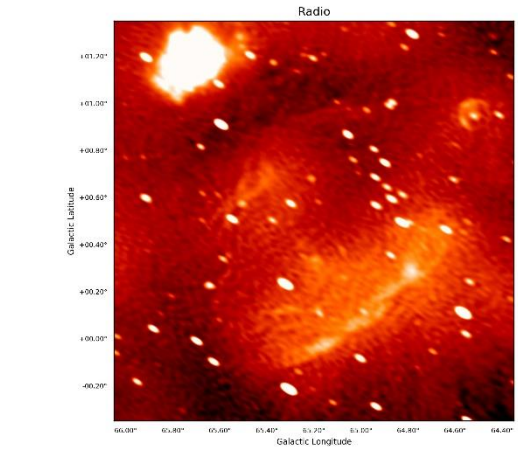
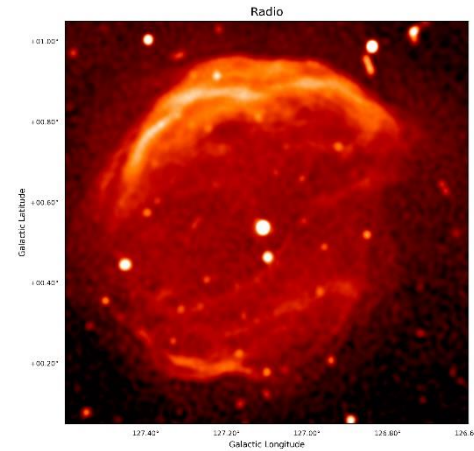


Future work

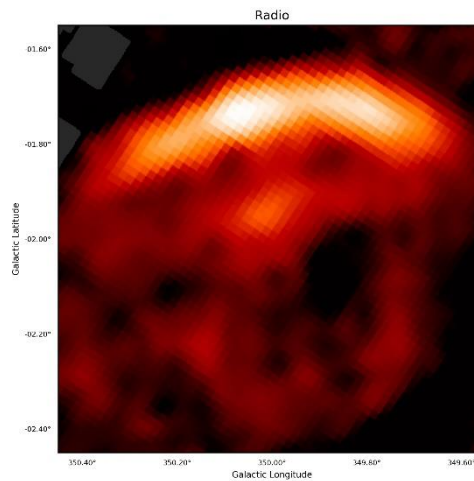


Next step is to create suitable scaling laws to allow measurement of:

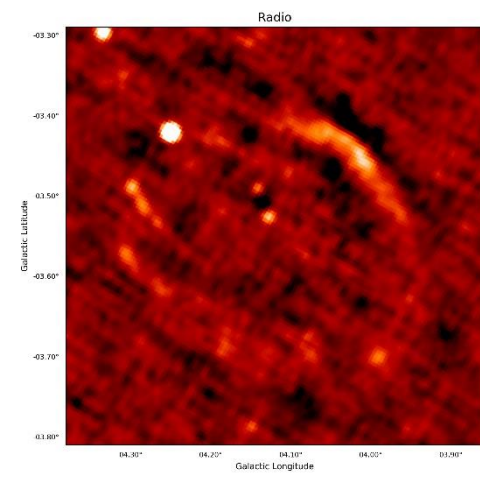
- Field strength
- Age
- Explosion energy
- Particle density



G06



G3



G00

Conclusions



- Blast waves deviate from Taylor-Sedov phase due to uniform magnetic field
 - Effects are visible when β is order unity, although due to deceleration already inherent in system this value will be reached at some point.
 - Symmetry axis of SNRs can be linked to large scale (Galactic) magnetic fields
 - Evidence that magnetic field fundamentally affects shock structure when $v_s \sim v_{ms}$
 - Future experiments could test MHD shock theory in controlled manner
-

Thank you for listening

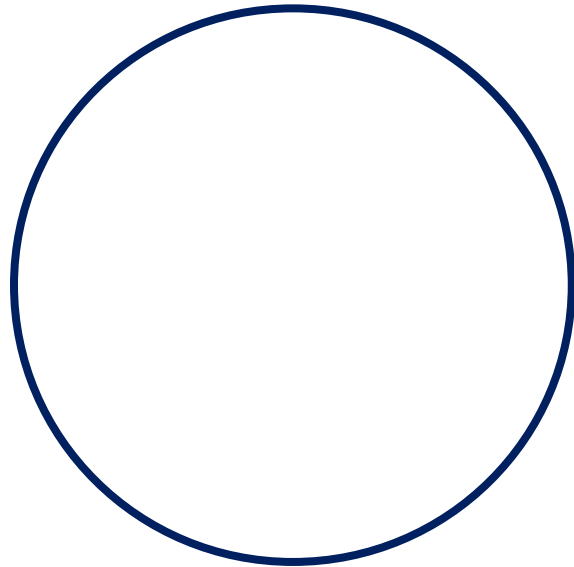


Questions

Barrel shaped blast wave



Without magnetic field



Magnetic field →

